Available online at www.sciencedirect.com

ScienceDirect

Nuclear Physics B 984 (2022) 115962

NUCLEAR PHYSICS B

www.elsevier.com/locate/nuclphysb

Heavy singly charged Higgs bosons and inverse seesaw neutrinos as origins of large $(g-2)_{e,\mu}$ in two Higgs doublet models

L.T. Hue [a,b], A.E. Cárcamo Hernández [c,d,e], H.N. Long [f], T.T. Hong [g,*]

[a] *Subatomic Physics Research Group, Science and Technology Advanced Institute, Van Lang University, Ho Chi Minh City 70000, Viet Nam*

[b] *Faculty of Applied Technology, School of Engineering and Technology, Van Lang University, Ho Chi Minh City 70000, Viet Nam*

[c] *Universidad Técnica Federico Santa María, Casilla 110-V, Valparaíso, Chile*

[d] *Centro Científico-Tecnológico de Valparaíso, Casilla 110-V, Valparaíso, Chile*

[e] *Millennium Institute for Subatomic Physics at High-Energy Frontier (SAPHIR), Fernández Concha 700, Santiago, Chile*

[f] *Institute of Physics, Vietnam Academy of Science and Technology, 10 Dao Tan, Ba Dinh, Hanoi 10000, Viet Nam*

[g] *An Giang University, VNU - HCM, Ung Van Khiem Street, Long Xuyen, An Giang 88000, Viet Nam*

Received 10 March 2022; received in revised form 11 July 2022; accepted 29 August 2022
Available online 9 September 2022
Editor: Tommy Ohlsson

Abstract

We show that simple extensions of two Higgs doublet models consisting of new heavy neutrinos and a singly charged Higgs boson singlet can successfully explain the experimental data on muon and electron anomalous magnetic moments thanks to large chirally-enhanced one-loop level contributions. These contributions arise from the large couplings of inverse seesaw neutrinos with singly charged Higgs bosons and right-handed charged leptons. The regions of parameter space satisfying the experimental data on $(g-2)_{e,\mu}$ anomalies allow heavy singly charged Higgs boson masses above the TeV scale, provided that heavy neutrino masses are above few hundred GeV, the non-unitary part of the active neutrino mixing matrix must be large enough, two singly charged Higgs bosons are non degenerate, and the mixing between singly charged Higgs bosons must be non-zero.

* Corresponding author.
E-mail addresses: lethohue@vlu.edu.vn (L.T. Hue), antonio.carcamo@usm.cl (A.E. Cárcamo Hernández), hnlong@iop.vast.vn (H.N. Long), tthong@agu.edu.vn (T.T. Hong).

https://doi.org/10.1016/j.nuclphysb.2022.115962

1. Introduction

The latest experimental measurement for the anomalous magnetic moment (AMM) of the muon $a_\mu \equiv (g-2)_\mu/2$ has been reported from Fermilab [1] and is in agreement with the previous experimental result measured by Brookhaven National Laboratory (BNL) E82 [2]. A combination of these results in the new average value of $a_\mu^{\rm exp} = 116592061(41) \times 10^{-11}$, which leads to the improved standard deviation of 4.2 σ from the Standard Model (SM) prediction, namely

$$\Delta a_\mu^{\rm NP} \equiv a_\mu^{\rm exp} - a_\mu^{\rm SM} = (2.51 \pm 0.59) \times 10^{-9}, \tag{1}$$

where $a_\mu^{\rm SM} = 116591810(43) \times 10^{-11}$ is the SM prediction [3] combined from various different contributions [4–24]. On the other hand, the recent experimental a_e data was reported from different groups [25–27], leading to the latest deviation between experiment and the SM prediction [19,28–33] as follows:

$$\Delta a_e^{\rm NP} \equiv a_e^{\rm exp} - a_e^{\rm SM} = (4.8 \pm 3.0) \times 10^{-13}. \tag{2}$$

Many Beyond Standard Model (BSM) theories have been constructed to explain the $(g-2)_{\mu,e}$ anomalies. Such theories rely on the inclusion of vector-like lepton multiplets [34–50], leptoquarks [51–54], both neutral and charged Higgs bosons as $SU(2)_L$ singlets [55,56]. Some two Higgs doublet models (THDM) can provide sizeable two-loop contributions to Δa_μ arising from new $SU(2)_L$ Higgs doublets [57–63,112], where some of them require rather light masses of new neutral and/or charged Higgs bosons at few hundred GeV.

There are many types of different versions of THDM, such as for instance: type I, type II, type X and type Y, which are discussed in Ref. [64], where collider phenomenology will give rise to different physical results. They are distinguished among themselves by the ways in which the two different $SU(2)_L$ Higgs doublets $\Phi_{1,2}$ generate the masses of up and down quarks as well as of charged leptons. These models arise from suitable choices of Z_2 charge assignments. The Yukawa couplings of Higgs bosons with heavy fermions will be constrained by the perturbative limits, for example $0.4 \leq \tan\beta \leq 91$ corresponding to the definitions of Yukawa couplings of the top and bottom quarks $|Y_t| = (\sqrt{2}/v) m_t \cot\beta < \sqrt{\pi}$ and $|Y_b| = (\sqrt{2}/v) m_b \tan\beta < \sqrt{\pi}$, where $\tan\beta$ is the ratio between the two vacuum expectations values (vevs) of the two neutral Higgs components. Discussions on the original THDM have shown that a new $SU(2)_L$ Higgs doublet can be used to accommodate the $(g-2)_{e,\mu}$ anomalies in a rather narrow allowed region of parameter space at the price of imposing dangerous requirements that can be experimentally tested in the near future [58,65]. The conclusion is also true for the Minimal Supersymmetric Model (MSSM) [66–68]. Another solution for MSSM requires large SUSY threshold corrections enough to change both sizes and signs of the SUSY electron and muon Yukawa couplings [69], hence allow regions satisfying both $(g-2)_{e,\mu}$ anomalies with large TeV scale of slepton masses, but rather large $t_\beta \geq 70$ is needed. As usual solution, there is a variety of extensions of THDM that successfully explain and accommodate the $(g-2)_{e,\mu}$ anomalies by adding new vector-like fermions as $SU(2)_L$ multiplets [38–43] as well as $SU(2)_L$ singlets of neutral and charged Higgs bosons [55,57,71–74]. Only few THDM models with scalar singlets and fermions can successfully explain the experimental data of both muon and electron anomalous magnetic

moments [42,70,72]. Our work here will introduce a more general solution that a wide class of the THDM by adding heavy right handed (RH) neutrino singlets and one singly electrically charged Higgs bosons can give sizeable one-loop contributions enough to explain the experimental ranges of values of both muon and electron anomalous magnetic moments in a wide region of parameter space.

This paper is organized as follows. In Sec. 2, the THDM extension with new RH neutrinos and singly charged Higgs boson (THDM$N_R h^{\pm}$) will be introduced, where we pay attention to the leptons, gauge bosons, and Higgs sectors, giving all physical states as well the couplings that may give large one-loop contributions to AMM. In Sec. 3, the simple inverse seesaw (ISS) and analytic formulas for one-loop contributions to AMM are constructed. Numerical discussion will be shown in details. Our main results will be collected in Sec. 4.

2. Review of the THDM$N_R h^{\pm}$

In this section we will focus on the analysis of the lepton sector of the THDM$N_R h^{\pm}$. For details of the quark sector of different types of the THDM, the reader is referred to Refs. [75,76]. The leptonic, quark and scalar spectrum with their assignments under the $SU(2)_L \times U(1)_Y$ gauge group are given by [75,76]:

$$\begin{aligned}
&L_a = \begin{pmatrix} \nu_{aL} \\ e_{aL} \end{pmatrix} \sim (2,-1); \quad Q_{aL} = \begin{pmatrix} u_{aL} \\ d_{aL} \end{pmatrix} \sim \left(2, \frac{1}{3}\right), \\
&e_{aR} \sim (1,-2); \quad u_{aR} \sim \left(1, \frac{4}{3}\right); \quad d_{aR} \sim \left(1, -\frac{2}{3}\right); \\
&N_{IR} \sim (1,0),\ a = 1,2,3,\ I = 1,2,...,6; \\
&\Phi_i = \begin{pmatrix} \phi_i^+ \\ \phi_i^0 \end{pmatrix} \sim (2,1),\ \langle \Phi_i \rangle = \begin{pmatrix} 0 \\ \frac{v_i}{\sqrt{2}} \end{pmatrix},\ i = 1,2; \\
&h^{\pm} \sim (1, \pm 2).
\end{aligned} \tag{3}$$

Note that we use the old convention for the defining the hypercharge via the original Gell-Mann-Nishijima relation:

$$Q = T_3 + \frac{1}{2}Y. \tag{4}$$

Here we add six new neutrino singlets to the leptonic spectrum of the model in order to implement the standard ISS mechanism. Furthermore, the model scalar sector is augmented by the inclusion of singly charged Higgs bosons, which allow to generate the new Yukawa interaction $\overline{(N_{IR})^c} e_{aR} h^+$ thus resulting in sizeable one-loop contributions to AMM.

One of the most important parameters introduced in the THDM is

$$t_\beta \equiv \tan\beta = \frac{v_2}{v_1},\ s_\beta \equiv \sin\beta,\ c_\beta \equiv \cos\beta. \tag{5}$$

We will also follow the notations $s_x \equiv \sin x$, $c_x \equiv \cos x$, and $t_x = s_x/c_x$ for any parameter x. Because the Yukawa couplings of up type quarks and Φ_2 are fixed, we always have a lower bound $t_\beta \geq 0.4$. In the THDM type I, all fermions couple with only Φ_2, hence no upper bounds for t_β arise. In the THDM type II and Y, all down type quarks and charged leptons couple with Φ_1, hence $t_\beta \leq 91$. In the type-X, the Yukawa coupling of tau with Φ_1 gives $t_\beta \leq 348$.

Table 1
$Z_2 \times Z_3$ charge assignments of the model type-A for the case I (II) with heavy neutrinos couplings with Φ_1 (Φ_2), $w = e^{i2\pi/3}$.

	Q_{aL}	u_{aR}	d_{aR}	L_a	e_{aR}	$N_{1,2,3R}$	$N_{4,5,6R}$	Φ_1	Φ_2	h^+
Z_2	-	-	-	1	1	1(-1)	-1(1)	1	-1	-1(1)
Z_3	w	w^2	w^2	w	w^2	1	w	w^2	w^2	w

The THDM type-II and type-X where lepton doublets couple with only Φ_1 are called THDM type-A. The corresponding lepton Yukawa terms are:

$$-\mathcal{L}_\ell^{\rm Y} = Y^e_{ab}\overline{e_{aR}}\Phi_1^\dagger L_b + Y^N_{k,Ia}\overline{N_{IR}}\,(i\sigma_2\Phi_k)^T\, L_a + \frac{1}{2}M_{N,IJ}\overline{N_{IR}}(N_{JR})^c + Y^h_{Ia}\overline{(N_{IR})^c}e_{aR}h^+ + \text{h.c.}, \tag{6}$$

where $a, b = 1, 2, 3$ are family indices; $k = 1, 2$; and $I = 1, 2, 3, ...6$ are the number of new neutral lepton singlets. A rough condition for the perturbative limit of Y^h is $|Y^h_{Ia}| < \sqrt{4\pi}$, and should be smaller for trusty values [77]. The Z_2 charges of N_{IR} and $h^\pm$ are always chosen to guarantee the Z_2 symmetry of Lagrangian (6). Using the Z_2 charge assignments discussed in Ref. [64], two Higgs triplets $\Phi_{1,2}$ have different Z_2 charges, therefore N_{IR} couple with only one of them. In addition, we can consider the inclusion of new Z_3 discrete symmetry in the model in order to forbid the quartic scalar interaction $\left[\left(\Phi_1^\dagger\Phi_2\right)^2 + \text{H.c.}\right]$ that generates active neutrino masses at the one-loop level [105]. This guarantees that the Yukawa couplings Y^h_{Ia} do not have suppressed constraints arising from the neutrino oscillation experimental data. The detailed assignments of the Z_2 and Z_3 charges are shown in Table 1. The Z_3 charges of leptons are chosen for the implementation of the ISS mechanism in the total neutrino mass matrix, namely: i) the charged lepton mass term always consists of Φ_1, ii) only N_{aR} ($a = 1, 2, 3$) generate non-zero Dirac mass term of neutrinos, iii) and only $N_{(a+3)R}$ couple with $h^\pm$. The Z_2 charges of quarks depend on which types of well-known THDMs, hence we do not list here. The Z_3 charges of all quarks have the same values as those of lepton doublets and charged lepton singlets. This guarantees that the quark Yukawa terms are consistent with those previously discussed.

Different from the well-known THDM, the model under considerations has a new kind of Yukawa couplings with singly charged Higgs boson $h^\pm$ and right-handed neutrinos N_I. In the SM, the vacuum stability around the Plank scale requires the quartic coupling in the Higgs potential close to zero, and the upper bound of the SM Higgs boson mass is very close to the experimental value, $M_h < 126$ GeV [106]. This problem can be solved in the model by adding new scalars such as in the THDM [107], and even with the models by adding neutrino gauge singlets [108–110]. The reason is that additional scalar couplings to Higgs doublets generating SM-like Higgs boson mass give positive one-loop contributions to the β-functions of the quartic couplings, hence the negative values of these couplings implying the vacuum instability will be relaxed at higher energy scale. This consequence still holds with the appearance of large Yukawa couplings of new fermions with Higgs doublets, which give negative one-loop contributions to the β-functions of the quartic couplings. On the other hand, the upper bounds of these Yukawa couplings are required besides their bounds from the perturbative and unitarity limits, previously discussed for THDM in refs. [111], for example. This situation also applies to the THDM$N_R h^\pm$ model under consideration. On the other hand, the appearance of the singly charged Higgs boson $h^\pm$ resulting on the Yukawa coupling matrix Y^h, which is irrelevant with any Higgs doublets.

Hence Y^h is not constrained by the requirement of vacuum stability. Furthermore, the quartic couplings of $h^\pm$ with Higgs doublets in the Higgs potential will result in the higher energy scale satisfying the vacuum stability.

In the THDM type-I and type-Y, where charged lepton couple with Φ_2, the first term of Eq. (6) should replace Φ_1 with Φ_2. We call them the THDM type-B and will discuss later that the qualitative results for AMM do not change. This model type including the model introduced in Ref. [42].

We also emphasize that the models under consideration including the Yukawa part discussed on Ref. [55] focusing on one particular case of $\Phi_k = \Phi_2$. As we will show that in our numerical analysis, the regions of the parameter space predicting $\Delta a_{e,\mu}$ consistent with the experimental data, favor small values of t_β, including the range $t_\beta \in [0.4,\ 10]$ which was not mentioned in Ref. [55].

Defining $\nu'_L = (\nu_1, \nu_2, \nu_3)^T_L$ and $N_R = (N_1, N_2, ..., N_6)^T_R$, we find the following leptonic mass terms:

$$-\mathcal{L}^{\text{mass}}_{\text{lepton}} = \frac{Y^e_{ab} v_1}{\sqrt{2}} \overline{e'_{aR}} e'_{bL} + \frac{1}{2} \left(\overline{(\nu'_L)^c} \quad \overline{N_R} \right) \mathcal{M}^\nu \begin{pmatrix} \nu'_L \\ (N_R)^c \end{pmatrix} + \text{h.c.},$$
$$\mathcal{M}^\nu = \begin{pmatrix} 0_{3\times 3} & M_D^T \\ M_D & M_N \end{pmatrix}, \tag{7}$$

where

$$(M_D)_{Ia} \equiv M_{D,Ia} = \sum_{k=1}^{2} \frac{Y^N_{k,Ia} v_k}{\sqrt{2}} \tag{8}$$

are the components of a 6×3 Dirac neutrino mass matrix and M_N is a 6×6 symmetric Majorana mass matrix. Here we choose basis where the charged lepton mass matrix is diagonal, which implies $Y^e_{ab} = \delta_{ab}\sqrt{2} m_{e_a}/v_1$, i.e., the flavor and mass states of charged leptons are the same. The total unitary mixing matrix is defined as

$$U^{\nu T} \mathcal{M}^\nu U^\nu = \hat{\mathcal{M}}^\nu = \text{diag}(m_{n_1},\ m_{n_2},\ ...,\ m_{n_9}) \equiv \text{diag}(\hat{m}_\nu,\ \hat{M}_N),$$
$$\begin{pmatrix} \nu'_L \\ (N_R)^c \end{pmatrix} = U^\nu n_L,\ \begin{pmatrix} (\nu'_L)^c \\ N_R \end{pmatrix} = U^{\nu *} n_R = U^{\nu *} (n_L)^c, \tag{9}$$

where $n_{L,R} = (n_1, n_2, ..., n_9)_{L,R}$ are the Majorana neutrino mass eigenstates satisfying $n_{iL,R} = (n_{iR,L})^c$, and the four-component forms are $n_i = (n_{iL}, n_{iR})^T$.

Given that we are working in the basis where the charged lepton mass matrix is diagonal, the leptonic mixing entirely arises from the neutrino sector. This implies that, in order to successfully reproduce the neutrino oscillation experimental data, the neutrino mixing matrix is parameterized in the following form [78]:

$$U^\nu = \begin{pmatrix} \left(I_3 - \frac{1}{2} R R^\dagger\right) U_{\text{PMNS}} & RV \\ -R^\dagger U_{\text{PMNS}} & \left(I_6 - \frac{1}{2} R^\dagger R\right) V \end{pmatrix} + \mathcal{O}(R^3), \tag{10}$$

where V is a 6×6 unitary matrix; R is a 3×6 matrix satisfying $|R_{aI}| < 1$ for all $a = 1, 2, 3$, and $I = 1, 2, ..., 6$. The 3×3 unitary matrix U_{PMNS} is the Pontecorvo-Maki-Nakagawa-Sakata (PMNS) matrix [79]. The condition $|R_{aI}| < 1$ needed to guarantee that the U^ν as a power series of R given in Ref. [78] is convergent and the approximation up to the order R^2 results in seesaw relations well-known in literature. Namely, the total neutrino mass matrix given in Eq. (7) will

result in three light masses for active neutrinos and new heavy neutrinos, $m_{n_{1,2,3}} \ll m_{n_{4,5,...}}$. This form of U^ν is consistent with many other well-known parameterizations [102–104].

The successful implementation of the ISS mechanism requires to construct the Dirac and Majorana mass matrices in terms of 3×3 submatrices as follows [78,80]

$$M_D^T = (m_D^T,\ 0_{3\times 3}), \qquad M_N = \begin{pmatrix} 0_{3\times 3} & M_R \\ M_R^T & \mu_X \end{pmatrix}, \tag{11}$$

where $0_{3\times 3}$ is the 3×3 null matrix. Using a new notation $M = M_R \mu_X^{-1} M_R^T$, we have the following ISS relations:

$$\begin{aligned} R = M_D^\dagger M_N^{*-1} &= \left(-m_D^\dagger M^{*-1}, \quad m_D^\dagger \left(M_R^\dagger\right)^{-1}\right), \\ U_{\rm PMNS}^* \hat{m}_\nu U_{\rm PMNS}^\dagger = m_\nu &= -M_D^T M_N^{-1} M_D = m_D^T \left(M_R^T\right)^{-1} \mu_X M_R^{-1} m_D, \\ V^* \hat{M}_N V^\dagger &\simeq M_N + \frac{1}{2} R^T R^* M_N + \frac{1}{2} M_N R^\dagger R. \end{aligned} \tag{12}$$

Because m_D is parameterized in terms of many free parameters, hence it is enough to choose $\mu_X = \mu_0 I_3$ with $\mu_0 > 0$, $M_R = \hat{M}_R = M_0 I_3$. We choose a simple form $m_D = \frac{M_0}{\sqrt{\mu_0}} \sqrt{\hat{m}_\nu} U_{\rm PMNS}^\dagger$ [78,80,81]. The ISS condition $|\hat{m}_\nu| \ll |\mu_X| \ll |m_D| \ll M_0$ gives $\frac{\sqrt{\mu_0 \hat{m}_\nu}}{M_0} \simeq 0$ and

$$\hat{M}_N = \begin{pmatrix} \hat{M}_R & 0_{3\times 3} \\ 0_{3\times 3} & \hat{M}_R \end{pmatrix} \simeq M_0 I_6,\ V \simeq \frac{1}{\sqrt{2}} \begin{pmatrix} -i I_3 & I_3 \\ i I_3 & I_3 \end{pmatrix}, \tag{13}$$

meaning that all of six heavy neutrinos have approximately the same mass $m_{n_i} \simeq M_0$ for all $i > 3$. Hence, the above simple forms of M_R, and μ_X will result in degenerate heavy neutrino masses, leading to small rates of lepton flavor violating decays of charged leptons (cLFV) that satisfy the current experimental constraints [82,83]. Relations in (12) reduce to the following simple forms:

$$m_D = M_0 \hat{x}_\nu^{1/2} U_{\rm PMNS}^\dagger, \quad R = \left(-U_{\rm PMNS} \frac{\sqrt{\mu_0 \hat{m}_\nu}}{M_0},\ U_{\rm PMNS} \hat{x}_\nu^{1/2}\right) \simeq \left(0_{3\times 3},\ U_{\rm PMNS} \hat{x}_\nu^{1/2}\right), \tag{14}$$

where

$$\hat{x}_\nu \equiv \frac{\hat{m}_\nu}{\mu_0} \equiv {\rm diag}\left(\hat{x}_{\nu 1}, \hat{x}_{\nu 2}, \hat{x}_{\nu 3}\right),\ \hat{x}_{\nu a} \equiv \frac{m_{n_a}}{\mu_0},\ a = 1,2,3 \tag{15}$$

satisfying $\max[|\hat{x}_{\nu a}|] \ll 1$ for all $a = 1,2,3$.

In our numerical analysis, we will use the best-fit values of the neutrino oscillation data [79] corresponding to the normal order (NO) scheme with $m_{n_1} < m_{n_2} < m_{n_3}$, namely

$$\begin{aligned} &s_{12}^2 = 0.32,\ s_{23}^2 = 0.547,\ s_{13}^2 = 0.0216,\ \delta = 218\ [{\rm Deg}], \\ &\Delta m_{21}^2 = 7.55 \times 10^{-5} [{\rm eV}^2],\ \Delta m_{32}^2 = 2.424 \times 10^{-3} [{\rm eV}^2]. \end{aligned} \tag{16}$$

In our numerical analysis, we have used the following relations

$$\hat{x}_\nu = \mu_0^{-1} {\rm diag}\left(m_{n_1},\ \sqrt{m_{n_1}^2 + \Delta m_{21}^2},\ \sqrt{m_{n_1}^2 + \Delta m_{21}^2 + \Delta m_{32}^2}\right),$$

$$U_{\rm PMNS} = \begin{pmatrix} c_{12}c_{13} & c_{13}s_{12} & s_{13}e^{-i\delta} \\ -c_{23}s_{12} - c_{12}s_{13}s_{23}e^{i\delta} & c_{12}c_{23} - s_{12}s_{13}s_{23}e^{i\delta} & c_{13}s_{23} \\ s_{12}s_{23} - c_{12}c_{23}s_{13}e^{i\delta} & -c_{23}s_{12}s_{13}e^{i\delta} - c_{12}s_{23} & c_{13}c_{23} \end{pmatrix}$$
$$\simeq \begin{pmatrix} 0.816 & 0.56 & 0.147e^{-i\delta} \\ -0.381 - 0.09e^{i\delta} & 0.555 - 0.062e^{i\delta} & 0.732 \\ 0.418 - 0.082e^{i\delta} & -0.61 - 0.056e^{i\delta} & 0.666 \end{pmatrix}. \quad (17)$$

These numerical values of neutrino masses satisfy the cosmological constraint arising from the Planck 2018 experimental data [84]: $\sum_{i=a}^{3} m_{n_a} \leq 0.12$ eV. In order to simplify our numerical analysis, we assume $m_{n_1} = 0.01\ \text{eV} < m_{n_2} < m_{n_3}$.

The other well-known numerical parameters are given in Ref. [79], namely

$$g = 0.652,\ \alpha_e = \frac{1}{137} = \frac{e^2}{4\pi},\ s_W^2 = 0.231,$$
$$m_e = 5 \times 10^{-4}\ \text{GeV},\ m_\mu = 0.105\ \text{GeV},\ m_W = 80.385\ \text{GeV}. \quad (18)$$

Also the inverted order (IO) scheme with $m_{n_3} < m_{n_1} < m_{n_2}$ can be considered in the similar way, but the qualitative results are the same with those from NO scheme, so we will not present here.

The non-unitary of the active neutrino mixing matrix $\left(I_3 - \frac{1}{2}RR^\dagger\right)U_{\rm PMNS}$ is constrained by other phenomenological aspects such as, for instance, electroweak precision tests, cLFV decays [85–87], thus leading to the following constraints

$$\eta \equiv \frac{1}{2}\left|RR^\dagger\right| < \eta_0 = \begin{pmatrix} 2 \times 10^{-3} & 3.5 \times 10^{-5} & 8. \times 10^{-3} \\ 3.5 \times 10^{-5} & 8 \times 10^{-4} & 5.1 \times 10^{-3} \\ 8 \times 10^{-3} & 5.1 \times 10^{-3} & 2.7 \times 10^{-3} \end{pmatrix}. \quad (19)$$

This constraint is consistent with the data popularly used in recent works discussion on the ISS framework [55,88,114]. The constraint on η may be more strict, depending on particular models. For example in the type III and inverse seesaw models, one has the constraint $|\eta_{aa}| \leq \mathcal{O}(10^{-4})$ [36,89]. In our numerical analysis, we will choose the values satisfying $|\eta_{33}| \leq 10^{-3}$, which are also consistent with the updated constraints on neutrino couplings discussed in Ref. [90,91], including the constraint from lepton universality previously discussed [113].

In the next section, we will discuss the model scalar potential as well as the one-loop contributions to $\Delta a_{\mu,e}$.

3. Higgs bosons and one-loop contributions to Δa_{e_a}

The Higgs potential satisfying the symmetry mentioned in this work is

$$V = \mu_1^2\Phi_1^\dagger\Phi_1 + \mu_2^2\Phi_2^\dagger\Phi_2 - \left(\mu_3^2\Phi_2^\dagger\Phi_1 + \text{H.c.}\right)$$
$$+ \frac{1}{2}\lambda_1\left(\Phi_1^\dagger\Phi_1\right)^2 + \frac{1}{2}\lambda_2\left(\Phi_2^\dagger\Phi_2\right)^2 + \lambda_3\left(\Phi_1^\dagger\Phi_1\right)\left(\Phi_2^\dagger\Phi_2\right) + \lambda_4\left(\Phi_1^\dagger\Phi_2\right)\left(\Phi_2^\dagger\Phi_1\right)$$
$$+ \lambda_h\left|h^+\right|^4 + \left|h^+\right|^2\left[\mu_h^2 + \lambda_8\Phi_1^\dagger\Phi_1 + \lambda_9\Phi_2^\dagger\Phi_2\right] + \left(\mu\epsilon_{\alpha\beta}\Phi_1^\alpha\Phi_2^\beta h^- + \text{H.c.}\right),$$

where the Z_2 soft breaking term $\left(\mu_3^2\Phi_2^\dagger\Phi_1 + \text{H.c.}\right)$ is kept in order to generate non-zero mass for the CP-odd neutral Higgs predicted in this model. The quartic term $\left(\Phi_2^\dagger\Phi_1\right)^2$ vanishes because of the Z_3 symmetry, whose assignments for the particle spectrum are given in Table 1.

Consequently, the one-loop contributions to active neutrino masses discussed in Ref. [105] do not appear in this case, implying that all entries of Y^h are not constrained by this condition. In general, μ_3, and μ can be complex, while the remaining parameters $\mu_{1,2}$, μ_h, and $\lambda_{1,2,3,4,8,9,h}$ are real [75,76]. In this work, all of these parameters and vacuum expectation values (vev) are assumed to be real, which corresponds to CP conservation.

It is easy to find the two minimization conditions of the Higgs potential, then inserting them into the Higgs potential in order to find the physical electrically charged scalars as follows:

$$\begin{aligned}
&\begin{pmatrix} G^\pm \\ H^\pm \end{pmatrix} = \begin{pmatrix} c_\beta & s_\beta \\ -s_\beta & c_\beta \end{pmatrix} \begin{pmatrix} \phi_1^\pm \\ \phi_2^\pm \end{pmatrix}, \\
&\begin{pmatrix} h_1^\pm \\ h_2^\pm \end{pmatrix} = \begin{pmatrix} s_\varphi & c_\varphi \\ c_\varphi & -s_\varphi \end{pmatrix} \begin{pmatrix} h^\pm \\ H^\pm \end{pmatrix}, \quad s_{2\varphi} = \frac{\sqrt{2}v\mu}{m^2_{h_2^+} - m^2_{h_1^+}}, \\
&m^2_{h_1^+,h_2^+} \equiv \frac{1}{2}\left[M^2_{H^+} + M^2_{33} \mp \sqrt{\left(M^2_{H^+} - M^2_{33}\right)^2 + 2v^2\mu^2} \right],
\end{aligned} \tag{20}$$

where $t_\beta \equiv \tan\beta = \dfrac{v_2}{v_1}$, $s_x \equiv \sin x$, $c_x \equiv \cos x$, $M^2_{H^+} = \frac{\mu_3^2}{s_\beta c_\beta} - \dfrac{1}{2}v^2\lambda_4$, $M^2_{33} = \mu_h^2 + \frac{v^2}{2}\left(c_\beta^2\lambda_8 + s_\beta^2\lambda_9\right)$. This result is consistent with the one obtained from the Higgs potential used in Ref. [75] after some transformations into a new Higgs basis and parameters. Namely, the two Higgs doublets Φ_i are changed into a new basis as follows:

$$\begin{pmatrix} H_1 \\ H_2 \end{pmatrix} = \begin{pmatrix} c_\beta & s_\beta \\ -s_\beta & c_\beta \end{pmatrix} \begin{pmatrix} \Phi_1 \\ \Phi_2 \end{pmatrix}, \tag{21}$$

which can be expanded around the minimum as shown below:

$$H_1 = \begin{pmatrix} G^+ \\ \dfrac{v + \varphi_1^0 + iG^0}{\sqrt{2}} \end{pmatrix}, \; H_2 = \begin{pmatrix} H^+ \\ \dfrac{\varphi_2^0 + iA}{\sqrt{2}} \end{pmatrix}, \tag{22}$$

where $v_1^2 + v_2^2 = v^2 = (246\,\text{GeV})^2$. In addition, the free parameters of the Higgs potential are transformed as follows $\mu_1^2c_\beta^2 + \mu_2^2s_\beta^2 - \mu_3^2 2s_\beta c_\beta \to \mu_1^2$, $\mu_1^2s_\beta^2 + \mu_2^2c_\beta^2 + \mu_3^2 2s_\beta c_\beta \to \mu_2^2$, $(\mu_1^2 - \mu_2^2)s_\beta c_\beta + \mu_3^2(c_\beta^2 - s_\beta^2) \to \mu_3^2$, $\lambda_8 c_\beta^2 + \lambda_9 s_\beta^2 \to \lambda_8$, $\lambda_8 s_\beta^2 + \lambda_9 c_\beta^2 \to \lambda_9$, $s_\beta c_\beta(\lambda_9 - \lambda_8) \to \lambda_{10}$, $\mu \to \mu$, ... The Higgs potential after the transformation (21) takes the form [75], where the physical charged scalar states and their masses are consistent with those ones given in Eq. (20).

In our numerical calculation, we will use $m^2_{h_k^+}$ and the mixing angle φ as free parameters. Three Higgs mass parameters μ_2^2, μ_h^2, and μ are functions of the remaining parameters. Thus, no perturbative limits on the Higgs selfcouplings are necessary to constrain the dependent functions chosen here.

From the above information we obtain all vertices providing one-loop contributions to the $e_b \to e_a\gamma$ decay rates as well as to Δa_{e_a}. They are collected from the lepton Yukawa terms given in Eq. (6) respecting all symmetries given in Table (1), namely

$$\mathcal{L}^{\text{yuk}}_{\text{lepton}} = -\frac{\sqrt{2}m_{e_a}}{v_1}\overline{L_a}\Phi_1^\dagger e_{aR} - Y^N_{k,ba}\overline{N_{bR}}\left(i\sigma_2\Phi_k\right)^T L_a - Y^h_{(b+3)a}\overline{(N_{(b+3)R})^c}e_{aR}h^+ + \text{h.c.}.$$

In order to derive the total neutrino mass matrix in the general ISS form, the leptonic Yukawa terms are rewritten as follows

$$\mathcal{L}^{\rm yuk}_{\rm lepton} = -\frac{g m_{e_a}(-t_\beta)}{\sqrt{2} m_W}\overline{L_a} H_2 e_{aR} - Y^N_{0,Ia}\overline{N_{IR}}\left(i\sigma_2 H_2\right)^T L_a - Y^h_{Ia}\overline{(N_{IR})^c} e_{aR} h^+ + \text{h.c.}, \tag{23}$$

where we denote $Y^N_0 \equiv \left(Y^N_0,\ 0_{3\times 3}\right)^T = -s_\beta Y^N_1 + c_\beta Y^N_2$ for the ISS mechanism discussed in this work. It is interesting to link this matrix with M_D given in Eq. (8), where depending on the Z_2 charges of N_{IR} there are two cases where non-zero couplings with only Φ_1 or Φ_2 correspond to $Y^N_2 = 0$ or $Y^N_1 = 0$, respectively. Namely

$$M^T_D = \left(\frac{v f^{-1}_H}{\sqrt{2}} Y^N_0,\ 0_{3\times 3}\right)^T,\ f_H = \begin{bmatrix} t^{-1}_\beta, & Y^N_1 = 0_{6\times 3},\ Y^N_2 \neq 0; \\ -t_\beta, & Y^N_2 = 0_{6\times 3},\ Y^N_1 \neq 0 \end{bmatrix}. \tag{24}$$

With this new notation, the Yukawa Lagrangian for the THDM type-A is

$$\begin{aligned}\mathcal{L}^{\rm yuk}_{\rm lepton} =& \frac{g m_{e_a} t_\beta}{\sqrt{2} m_W} U^{\nu *}_{ai}\overline{n_{iL}} e_{aR}\left(c_\varphi h^+_1 - s_\varphi h^+_2\right) \\ &+ \frac{g f_H}{\sqrt{2} m_W} U^\nu_{(I+3)i} M_{D,ia}\overline{n_{iR}} e_{aL}\left(c_\varphi h^+_1 - s_\varphi h^+_2\right) \\ &- Y^h_{Ib} U^{\nu *}_{(I+3)i}\overline{n_{iL}} e_{aR}\left(s_\varphi h^+_1 + c_\varphi h^+_2\right) + \text{h.c.}.\end{aligned} \tag{25}$$

Then, all relevant couplings are given in the following lepton Yukawa interaction Lagrangian

$$\mathcal{L} = \sum^3_{a=1}\sum^9_{i=1}\left[\frac{g}{\sqrt{2} m_W}\sum^2_{k=1}\overline{n_i}\left(\lambda^{L,k}_{ia} P_L + \lambda^{R,k}_{ia} P_R\right) e_a h^+_k + \frac{g}{\sqrt{2}} U^{\nu *}_{ai}\overline{n_i}\gamma^\mu P_L e_a W^+_\mu\right] + \text{h.c.}, \tag{26}$$

where

$$\begin{aligned}\lambda^{L,1}_{ia} &= \sum^6_{I=1} f_H M_{D,Ia} c_\varphi U^\nu_{(I+3)i} \simeq f_H c_\varphi \times \begin{bmatrix} 0, & i \leq 3 \\ \left(M^T_D V\right)_{a(i-3)}, & i > 3 \end{bmatrix}, \\ \lambda^{L,2}_{ia} &\simeq -\lambda^{L,1}_{ia} t_\varphi = \lambda^{L,1}_{ia}\left[c_\varphi \to -s_\varphi\right], \\ \lambda^{R,1}_{ia} &= m_{e_a} t_\beta c_\varphi U^{\nu *}_{ai} - \sum^6_{I=1}\frac{v}{\sqrt{2}} s_\varphi Y^h_{Ia} U^{\nu *}_{(I+3)i} \\ &\simeq \begin{bmatrix} m_{e_a} t_\beta c_\varphi\left[U^*_{\rm PMNS}\left(I_3 - \frac{1}{2}\hat{x}_\nu\right)\right]_{ai} + \frac{v s_\varphi}{\sqrt{2}}\left(Y^{hT} R^T U^*_{\rm PMNS}\right)_{ai}, & i \leq 3 \\ m_{e_a} t_\beta c_\varphi (RV)^*_{a(i-3)} - \frac{v s_\varphi}{\sqrt{2}}\left[Y^{hT}\left(I_6 - \frac{1}{2} R^T R^*\right) V^*\right]_{a(i-3)} & i > 3 \end{bmatrix}, \\ \lambda^{R,2}_{ia} &= -m_{e_a} t_\beta s_\varphi U^{\nu *}_{ai} - \sum^6_{I=1}\frac{v}{\sqrt{2}} c_\varphi Y^h_{Ia} U^{\nu *}_{(I+3)i} \\ &\simeq \begin{bmatrix} -m_{e_a} t_\beta s_\varphi\left[U^*_{\rm PMNS}\left(I_3 - \frac{1}{2}\hat{x}_\nu\right)\right]_{ai} + \frac{v c_\varphi}{\sqrt{2}}\left(Y^{hT} R^T U^*_{\rm PMNS}\right)_{ai}, & i \leq 3 \\ -m_{e_a} t_\beta s_\varphi (RV)^*_{a(i-3)} - \frac{v c_\varphi}{\sqrt{2}}\left[Y^{hT}\left(I_6 - \frac{1}{2} R^T R^*\right) V^*\right]_{a(i-3)} & i > 3 \end{bmatrix} \\ &= \lambda^{R,1}_{ia}\left[s_\varphi \to c_\varphi,\ c_\varphi \to -s_\varphi\right].\end{aligned} \tag{27}$$

The Feynman diagrams giving one-loop contributions to $(g-2)_{e_a}$ corresponding to the Lagrangian (26) are shown in Fig. 1.

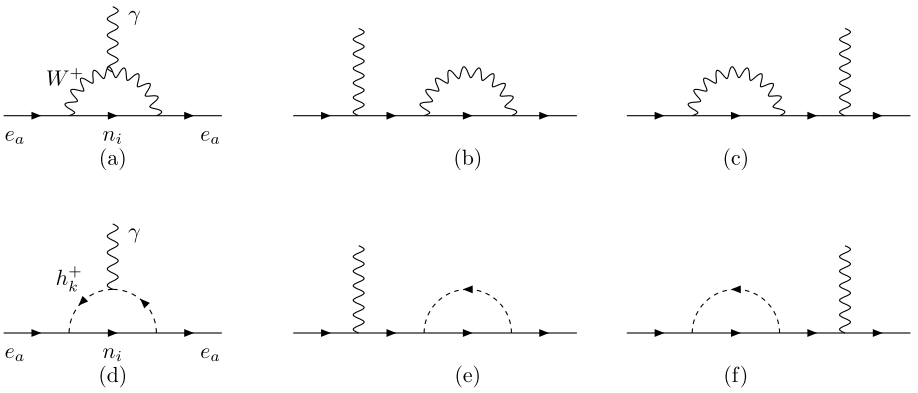

Fig. 1. One-loop contributions of $W^{\pm}$ and $h_k^{\pm}$ to $(g-2)_{e_a}$ in the unitary gauge, where $k = 1, 2$.

We do not list here the couplings of neutral gauge and Higgs bosons because they give suppressed contributions to $a_{e_a}^{\rm NP}$. In particular, the relevant couplings are only the ones with usual charged leptons $s^0\overline{e_a}e_a$ and $Z_\mu\overline{e_a}\gamma^\mu e_a$. The one-loop level contribution arising from the Z gauge boson exchange is the same as the predicted by the SM. The contributions arising from new neutral Higgs bosons are not larger than the one coming from the SM-like Higgs boson since they are suppressed by a factor of the order of $\mathcal{O}(10^{-14})$, because we assume here their masses are at the TeV scale.

We will use the approximation that $m_{n_i}^2/m_W^2 = 0$ with $i \leq 3$ and $m_{n_i}^2/m_W^2 = M_0^2/m_W^2 = x_W$ with $i > 3$. Then, the contribution to a_{e_a} arising from the W exchange has the form:

$$a_{e_a}(W) = -\frac{g^2 m_{e_a}^2}{8\pi^2 m_W^2}\left[-\frac{5}{12} + \left(R^* R^T\right)_{aa} \times \left(\tilde{f}_V(x_W) + \frac{5}{12}\right)\right], \tag{28}$$

where

$$\tilde{f}_V(x) = \frac{-4x^4 + 49x^3 - 78x^2 + 43x - 10 - 18x^3 \ln x}{24(x-1)^4},$$
$$\tilde{f}_V(0) = -\frac{5}{12} \leq \tilde{f}_V(x) \leq \tilde{f}_V(\infty) = -\frac{1}{6}. \tag{29}$$

Because $|\tilde{f}_V(x_W) + \frac{5}{12}| \leq \frac{5}{12}$ and $\left(R^* R^T\right)_{aa} \leq \mathcal{O}(10^{-3}) \ll 1$, Eq. (28) equals to the one-loop level contribution predicted by the SM, see example in Ref. [92]:

$$a_\mu^{(1)\rm SM}(W) = \frac{g^2 m_\mu^2}{8\pi^2 m_W^2} \times \frac{5}{12} \simeq 383 \times 10^{-11}, \ \frac{g^2 m_\mu^2}{8\pi^2 m_W^2} \simeq 9.19 \times 10^{-9}. \tag{30}$$

The one-loop level contribution to Δa_{e_a} arising from the exchange of the electrically charged scalar singlet $h_k^{\pm}$ is given by [35]:

$$a_{e_a}(h_k^{\pm}) = -\frac{g^2 m_{e_a}}{8\pi^2 m_W^2}\sum_{i=1}^{9}\frac{\lambda_{ia}^{L,k*}\lambda_{ia}^{R,k} m_{n_i} f_\Phi(x_{i,k}) + m_{e_a}\left(\lambda_{ia}^{L,k*}\lambda_{ia}^{L,k} + \lambda_{ia}^{R,k*}\lambda_{ia}^{R,k}\right)\tilde{f}_\Phi(x_{i,k})}{m_{h_k^{\pm}}^2}, \tag{31}$$

where $x_{i,k} \equiv m_{n_i}^2/m_{h_k^{\pm}}^2$ and the loop functions appearing in Eq. (31) have the forms:

$$f_\Phi(x)=\frac{x^2-1-2x\ln x}{4(x-1)^3},\quad \tilde{f}_\Phi(x)=\frac{2x^3+3x^2-6x+1-6x^2\ln x}{24(x-1)^4},$$
$$f_\Phi(\infty)=0\leq f_\Phi(x)\leq f_\Phi(0)=\frac{1}{4},\ \tilde{f}_\Phi(\infty)=0\leq \tilde{f}_\Phi(x)\leq \tilde{f}_\Phi 0)=\frac{1}{24}. \tag{32}$$

And the deviation from the SM is defined as follows:

$$\Delta a_{e_a}=\sum_{k=1}^{2}a_{e_a}(h_k^\pm)+\Delta a_{e_a}(W),\ \Delta a_{e_a}(W)\equiv a_{e_a}(W)-a_{e_a}^{(1)\mathrm{SM}}(W), \tag{33}$$

where $a_\mu^{(1)\mathrm{SM}}(W)\simeq 3.83\times 10^{-9}$ [92].

Using the approximations $m_{n_i}^2/m_{h_k^\pm}^2\simeq 0$ for $i\leq 3$ and $m_{n_i}^2/m_{h_k^\pm}^2\simeq M_0^2/m_{h_k^\pm}^2=x_k$, we have $f_\Phi(x_{i,k})\simeq f_\Phi(0)$ for $i\leq 3$ and $f_\Phi(x_{i,k})\simeq f_\Phi(x_k)$ for $i>3$. Following Eqs. (13) and (14), we obtain that the one loop level contribution to a_{e_a} due to the exchange of $h_1^\pm$ is given by

$$\begin{aligned}
a_{e_a}(h_1^\pm)=&-9.19\times 10^{-9}\times\frac{m_{e_a}^2}{m_\mu^2}\\
&\times\mathrm{Re}\left\{\sum_{c=1}^{3}f_H\left[c_\varphi^2 t_\beta\left|U_{\mathrm{PMNS},ac}\right|^2\frac{m_{n_c}}{\mu_0}\right.\right.\\
&\left.-\frac{vc_\varphi s_\varphi}{\sqrt{2}m_{e_a}}U_{\mathrm{PMNS},ac}\left(\frac{m_{n_c}}{\mu_0}\right)^{1/2}Y^h_{(c+3)a}\right]x_1 f_\Phi(x_1)\\
&+\sum_{c=1}^{3}\left[\left|U_{\mathrm{PMNS},ac}\right|^2\left(f_H^2c_\varphi^2\frac{m_{n_c}}{\mu_0}\right)\right]x_1\tilde{f}_\Phi(x_1)\\
&+\frac{m_{e_a}^2t_\beta^2c_\varphi^2}{m_{H_1^\pm}^2}\left[\frac{1}{24}-\sum_{c=1}^{3}\left[\left|U_{\mathrm{PMNS},ac}\right|^2\frac{m_{n_c}}{\mu_0}\right]\left(\frac{1}{24}-\tilde{f}_\Phi(x_1)\right)\right]\\
&+\frac{v^2s_\varphi^2}{2m_{H_1^\pm}^2}\left[\sum_{c=1}^{3}\left[\left|Y^h_{(c+3)a}\right|^2\frac{m_{n_c}}{\mu_0}\right]\left(\frac{1}{24}-\tilde{f}_\Phi(x_1)\right)+\left(Y^{h\dagger}Y^h\right)_{aa}\tilde{f}_\Phi(x_1)\right]\\
&\left.-\frac{vm_{e_a}t_\beta s_{2\varphi}}{\sqrt{2}m_{H_1^\pm}^2}\left(\frac{1}{24}-\tilde{f}_\Phi(x_1)\right)\sum_{c=1}^{3}\left[U_{\mathrm{PMNS},ac}Y^h_{(c+3)a}\left(\frac{m_{n_c}}{\mu_0}\right)^{1/2}\right]\right\},
\end{aligned} \tag{34}$$

$$a_{e_a}(h_2^\pm)=a_{e_a}(h_1^\pm)\left[x_1\to\ x_2,\ s_\varphi\to c_\varphi,\ c_\varphi\to -s_\varphi\right]. \tag{35}$$

In the real part of Eq. (34), the first line corresponds to the chirally-enhanced part proportional to $\lambda^{L,1*}\lambda^{R,1}$ whereas the second and remaining lines are the parts proportional to $\lambda^{L,1*}\lambda^{L,1}$ and $\lambda^{R,1*}\lambda^{R,1}$, respectively.

Now we compare our results given in Eq. (34) with the one-loop contribution due to the exchange of singly electrically charged Higgs bosons in the original versions [64] without N_{IR} and the singlet $h^\pm$. Now we assume $h_1^\pm\equiv H^\pm$ in Eq. (20), corresponding to $c_\varphi=1, s_\varphi=0$. The absence of N_{IR} can be conveniently derived from $f_H=0$ and $f(x_1)=0$, thus implying that the only one-loop contribution from $h_1^\pm$ only consists of the first term in the third line of the real part given in Eq. (34), which is proportional to $-9.19\times 10^{-9}\times m_{e_a}^4t_\beta^2c_\varphi^2/(24m_\mu^2m_{H_1^\pm}^2)$, which yields

a small and negative contribution to $\Delta a_\mu^{\rm NP}$ [65]. The dominant contributions to AMM arise from two-loop Barr-Zee type diagrams. The similar conclusion for the THDM type-B where $t_\beta^2 \to t_\beta^{-2}$, hence has suppressed two-loop contributions to AMM for $t_\beta \geq 0.4$.

If the mixing between two singly charged Higgs bosons vanishes, namely $s_\alpha c_\alpha = 0$, then all of the remaining terms in both Eqs. (34) and (35) are negative, thus not allowing to accommodate the experimental data on muon and electron anomalous magnetic moments.

Using the constraint (19) for $RR^\dagger = U_{\rm PMNS}\hat{x}_\nu U_{\rm PMNS}^\dagger$ we have $\hat{x}_\nu < \mathcal{O}(10^{-3})$. Therefore, we will choose a safe upper bound as follows

$$\hat{x}_{\nu 3} \equiv \left(\hat{x}_\nu\right)_{33} = \frac{m_{n_3}}{\mu_0} \leq 10^{-3}. \tag{36}$$

To avoid unnecessary independent parameters of Y^h_{Ia} without any qualitative AMM results discussed on this work and in order to cancel large one-loop contributions from these Higgs bosons to the cLFV decays $e_b \to e_a\gamma$, we assume that

$$\sum_{c=1}^{3} U_{{\rm PMNS},ac}\left(\frac{m_{n_c}}{m_{n_3}}\right)^{1/2} Y^h_{(c+3)b} = Y^d_a \delta_{ab}\,. \tag{37}$$

The total one-loop level contribution arising from the exchange of two singly charged Higgs bosons is written as

$$a_{e_a}(h^\pm) \equiv a_{e_a}(h_1^\pm) + a_{e_a}(h_2^\pm) = a_{e_a,0}(h^\pm) + \ldots, \tag{38}$$

$$a_{e_a,0}(h^\pm) = 9.19\times 10^{-9} f_H \times \frac{m_{e_a}^2}{m_\mu^2} \times {\rm Re}\left\{\frac{v s_{2\varphi}}{2\sqrt{2}m_{e_a}} \hat{x}_{\nu 3}^{1/2} Y_a^d \left[x_1 f_\Phi(x_1) - x_2 f_\Phi(x_2)\right]\right\}, \tag{39}$$

where $a_{e_a,0}(h^\pm)$ denotes the dominant term of the chirally-enhanced part coming from the second one in the first line of the real part given in Eq. (34) where x_k is the part relating with the contribution from $h_k^\pm$ exchange. This conclusion can be qualitatively understood from the property of the large factor $v/(2\sqrt{2}m_{e_a})$ as well as large free Yukawa couplings up to the perturbative limit $\max[|Y^h_{Ia}|] \leq \sqrt{4\pi}$. In addition, the sign of this term can be the same as $\Delta a_{e_a}^{\rm NP}$ depending on the sign of ${\rm Re}[Y_a^d]$ when all other factors are fixed. As a result, this term can easily explain both signs of $\Delta a_\mu^{\rm NP}$ and $\Delta a_e^{\rm NP}$ that are still in conflict between different experimental results and needed to be confirmed in the future. Our numerical investigation showed that the term in Eq. (39) is the dominant one, and the sum of all the remaining terms is suppressed in the allowed regions of parameter space. More detailed estimations confirming that the remaining contributions are suppressed were given in Ref. [100]. Finally, $a_{e_a,0}(h^\pm) \neq 0$ only when the mixing between two $SU(2)_L$ doublets and singlets is non-zero $s_\varphi c_\varphi \neq 0$, and their masses are non degenerate $m_{h_1^\pm} \neq m_{h_2^\pm}$.

We comment here an important property that $a_{e_a,0}(h^\pm)$ in Eq. (39) keeps the same form for both types of THDM A and B, because these models control only the first term of λ^R_{ia} in Eq. (27), which is proportional to t_β or t_β^{-1}. This key factor controls loop contributions to AMM, which are proportional to suppressed power of t_β^{-1} with large t_β in THDM of type-B, including the model type-I. Hence, it is impossible to accommodate the AMM data in the original version of the THDM type I. On the other hand, the THDM type-A has one and two loop contributions to AMM consisting of much enhanced factors of t_β^2 and t_β^4, respectively. Therefore, original

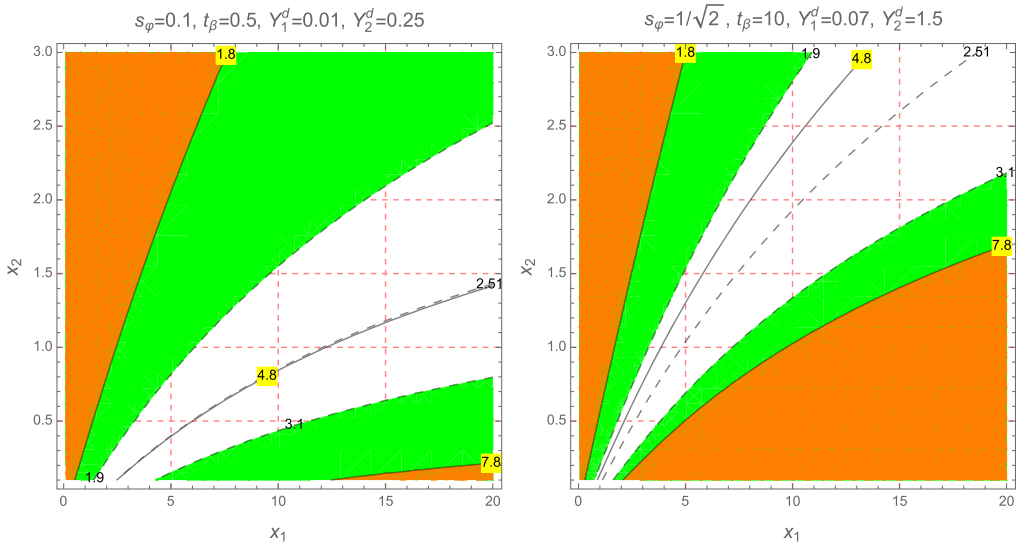

Fig. 2. Contour plots of $\Delta a_\mu(h^\pm) \times 10^9$ and $\Delta a_e(h^\pm) \times 10^{13}$ as functions of x_1 and x_2, where $\hat{x}_{\nu 3} = 10^{-3}$ and $f_H = t_\beta^{-1}$. The green (orange) regions are excluded by the 1σ data of $\Delta a_\mu^{\rm NP}$ ($\Delta a_e^{\rm NP}$). The black and dashed-black curves show the constant values of $\Delta a_e(h^\pm) \times 10^{13}$ and $\Delta a_\mu(h^\pm) \times 10^9$, respectively.

versions can predict large loop contributions to AMM, provided that the new Higgs bosons are light having low masses of about few hundred GeV. These might be excluded by future collider experiments. Then, the presence of $a_{e_a,0}(h^\pm)$ is an alternative way to explain the AMM data.

Now we consider the case of $f_H = t_\beta^{-1}$, which corresponds to the models where the RH neutrino singlets couple with Φ_2, whereas the charged leptons couple with Φ_1 [58,100]. Now, increasing values of $a_{e_a,0}(h^\pm)$ in Eq. (39) require small t_β values, thus implying that the scanning range of t_β should be chosen from the lower bound $t_\beta \geq 0.4$. Numerical illustrations of $a_{e_a,0}(h^\pm)$ are shown in Fig. 2 with fixed $\hat{x}_{\nu 3} = 10^{-3}$, i.e., $0 \neq |(Y_2^N)_{ab}| < \sqrt{4\pi}$. In addition, there are different fixed values of s_φ, t_β, Y_1^d, and Y_2^d shown in the respective panels, namely small $t_\beta = 0.5$ and large $t_\beta = 10$. We have checked that $a_{e_a,0}(h^\pm) \simeq a_{e_a}(h^\pm)$. Now we estimate the allowed ranges of M_0, $m_{h^\pm_{1,2}}$, which are affected from the perturbative limit of the Yukawa coupling matrix Y_0^N defined in Eq. (24) and related with M_0 through Eqs. (11), (8), and (14). We have two different constraints corresponding to $f_H = t_\beta^{-1}$ and $(-t_\beta)$. The constraint for $f_H = t_\beta^{-1}$ is

$$M_0 \left| \left(\hat{x}_\nu^{1/2} U_{\rm PMNS}^\dagger \right)_{ab} \right| = \frac{v t_\beta}{\sqrt{2}} \left| c_\beta (Y_2^N)_{(a+3)b} \right| < \frac{v s_\beta}{\sqrt{2}} \sqrt{4\pi}. \tag{40}$$

We can choose a more strict upper bound of $M_0 \leq \hat{x}_{\nu 3}^{-1/2} s_\beta v \sqrt{\pi/2} = 9.7 s_\beta$ TeV for $f_H = t_\beta^{-1}$ and $\hat{x}_{\nu 3} = 10^{-3}$. Therefore for $\hat{x}_{\nu 3} \leq 10^{-3}$ and $t_\beta \geq 0.4$, values of $M_0 \leq 6.4$ TeV are always acceptable. Applying this constraint, we consider a benchmark where $M_0 = 3$ TeV in order to estimate the allowed values of $m_{h^\pm_{1,2}}$. We can see that in the left-panel of Fig. 2, the range $0.2 \leq x_2 = M_0^2/m_{h_2^\pm}^2 \leq 1.5$ with $x_1 = M_0^2/m_{h_1^\pm}^2 = 10$ is allowed with respect to 2.5 TeV $\leq m_{h_2^\pm} \leq 5$ TeV and $m_{h_1^\pm} \simeq 0.95$ TeV. Similarly for the right panel of Fig. 2, we can choose $M_0 = 5$ TeV and larger $m_{h_2^\pm} = M_0/\sqrt{2.5}$ and $m_{h_1^\pm} \geq 5/\sqrt{15} > 1$ TeV.

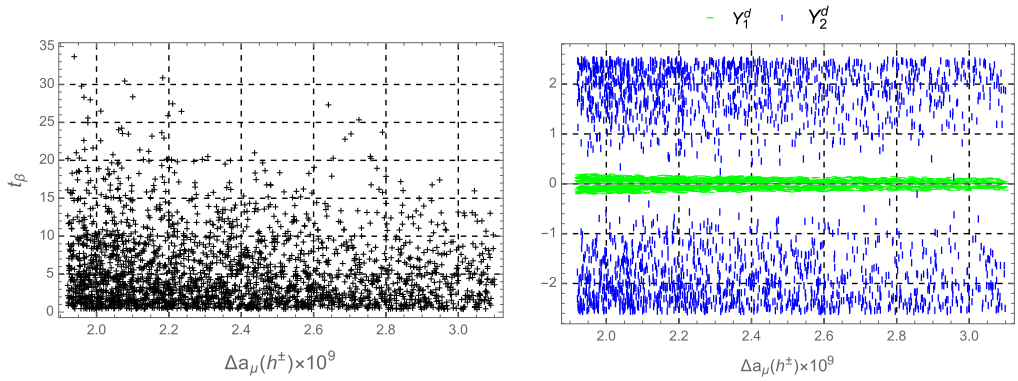

Fig. 3. The correlations of $\Delta a_\mu(h^\pm)$ vs t_β and $Y^d_{1,2}$ with $f_H = t_\beta^{-1}$.

In the last discussion we will focus on the allowed regions consisting of masses of heavy neutrinos and singly charged Higgs bosons below few TeV so that they can be detected by future colliders. The allowed regions are defined as they result in the two values of $\Delta a_\mu(h^\pm)$ and $\Delta a_e(h^\pm)$ both satisfying the experimental data of the muon and electron anomalous magnetic moments within the 1 σ level, and all perturbative limits of the Yukawa couplings Y^h_{Ia} and Y^N_{Ia} are satisfied, namely $|Y^h_{Ia}|, |Y^N_{2,Ia}| < \sqrt{4\pi}$. The region of parameter space used to scan is chosen as follows:

$$
\begin{aligned}
&0.8\ \text{TeV} \leq m_{h_1^\pm}, m_{h_2^\pm} \leq 5\ \text{TeV};\ 10\ \text{GeV} \leq M_0 \leq\ 5\ \text{TeV};\\
&0.3 \leq t_\beta \leq 50;\ \left|s_\varphi\right| \leq 1;\ |Y^d_{ab}| \leq 3;\ 10^{-7} \leq\ \hat{x}_{\nu 3} \equiv \left(\hat{x}_\nu\right)_{33} = \frac{m_{n_3}}{\mu_X} \leq 10^{-3}.
\end{aligned}
\tag{41}
$$

Here we fix $m_{n_1} = 0.01$ eV corresponding to the NO scheme used in our numerical analysis. Smaller values of m_{n_1} will result in small allowed ranges of $Y^d_{1,2}$ because of the perturbative limit affecting the relation given in Eq. (37). The scanned range of $\hat{x}_{\nu 3}$ satisfies the non-unitary constraint given in Eq. (19). The numerical results confirm that $\left|a_{e_a,0}(h^\pm)/a_{e_a}(h^\pm)\right| \simeq 1$, namely $0.995 < \left|a_{e,0}(h^\pm)/a_e(h^\pm)\right| < 1.005$ and $1 \leq \left|a_{\mu,0}(h^\pm)/a_\mu(h^\pm)\right| \leq 1.03$. Hence the discussion about correlations between different contributions in Eq. (35) will not be shown. The correlations between important free parameters vs. $\Delta a_\mu(h^\pm)$ are shown in Fig. 3. As mentioned above, large t_β favors small $\Delta a_\mu(h^\pm)$, leading to an upper bound on t_β in the allowed regions, see the left-panel of Fig. 3. The scanned ranges in Eq. (41) allow all experimental ranges of $\Delta a_{e,\mu}$. In addition, the dependence between Δa_e and Δa_μ is not interesting. We know instead that $\Delta a_e(h^\pm) \simeq \Delta a_{e,0}(h^\pm)$ is a function of the Yukawa coupling Y^d_1. Hence, the dependence of $\Delta a_e(h^\pm)$ on $\Delta a_\mu(h^\pm)$ can be seen from the dependence of the Yukawa coupling Y^d_1 in the right panel, where it is bounded in a more restrictive range than the one given in Eq. (41), see Table 2, where other allowed ranges are also listed.

As we mentioned above, the dominant contributions to Δa_{e_a} are $\Delta a_{e_a,0}$ given in Eq. (39). This property can be seen in Fig. 4, showing the dependence of the ratio Y^d_1/Y^d_2 and $Y^d_{1,2}$ on Δa_e. The allowed region of this ratio $Y^d_1/Y^d_2 \sim \Delta a_{e,0}(h^\pm)/\Delta a_{\mu,0}(h^\pm)$ also linearly depends on $\Delta a_e(h^\pm)$. The vertical width of the allowed region is controlled by both 1σ ranges of $\Delta a_e(h^\pm)$ and $\Delta a_\mu(h^\pm)$. Also, the right panel shows the linear dependence of the allowed region of Y^d_1 on

Table 2
Allowed ranges corresponding to the scanned region given in Eq. (41), considered in case of $f_H = t_\beta^{-1}$.

	t_β	$\|s_\varphi\|$	M_0 [GeV]	$\left\|Y_1^d\right\|$	$\left\|Y_2^d\right\|$	$\hat{x}_{\nu 3}$
Min	0.4	0.03	282	0.003	0.171	2.92×10^{-7}
Max	33.7	0.999	5000	0.203	2.529	10^{-3}

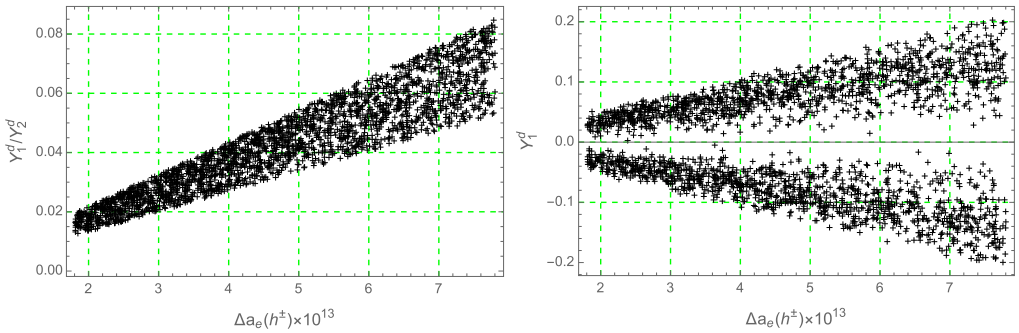

Fig. 4. $\frac{Y_1^d}{Y_{d2}^d}$ (left panel) and Y_1^d (right panel) as functions of Δa_e with $f_H = t_\beta^{-1}$.

$\Delta a_e(h^\pm)$. The linear behavior of Y_2^d is less clear than the one of Y_1^d because Y_2^d is also affected by the perturbative condition.

An interesting property is that excepting t_β, all other parameters like M_0, the non-unitary parameter $\hat{x}_{\nu 3}$, $Y_{1,2}^d$, and s_φ must have lower bounds. The allowed ranges of heavy neutrino masses $M_0 \geq \mathcal{O}(100)$ GeV might be confirmed by recent experimental searches in colliders such as LHC and ILC [94–98]. Because of the sizeable mixing angle $\sim \sqrt{x_{\nu,3}}$ between ISS and active neutrinos ν_{aL}, the main production channel of heavy neutrinos n_I (I=4,...,9) with mass M_0 at the LHC is via the Drell Yan anihilation process $u\bar{d} \to n_I e_a^+$ mediated by the W gauge boson in the s channel. Then the decay channel of n_I can be $n_I \to e_a^- W^+, n_a Z, n_a h$, where h is the standard model-like Higgs boson. The ILC can produce heavy neutrino in the processes $e^+e^- \to \bar{n}_a n_I$ through the exchange of virtual W and Z bosons in the t and s-channels, respectively. The model under consideration also predicts the production channel of a heavy neutrino pair $e^+e^- \to \bar{n}_I n_I$ through the virtual exchange of $h_k^\pm$. In addition, the singly charged Higgs bosons in the model under consideration can be searched in a proton-proton collider through the processes $pp \to \gamma^*/Z^* \to h_k^+ h_l^- \to (e_c^+ n_a)(\bar{n}_b e_d^-)$ (with $a, b, c, d = 1, 2, 3$), where the Yukawa couplings Y^h give an important contribution [115]. The ILC can produce two singly charged Higgs bosons $e^+e^- \to h_k^+ h_l^-$ through the n_I exchange in the t-channel. Studying these processes are beyond the scope of this work, but will be investigated in more detail elsewhere. Because of the non-vanishing mixing between $h^\pm$ and the singly charged components of the Higgs doublets, another decay into a CP-odd neutral Higgs boson A, such as $h_k^\pm \to A W^\pm$, can occur [112].

The correlations relating the masses with $\Delta a_\mu(h^\pm)$ are shown in Fig. 5. We can see that $m^2_{h_1^\pm}$ must be different than $m^2_{h_2^\pm}$ and our numerical analysis indicates $\left|m^2_{h_2^\pm} - m^2_{h_1^\pm}\right| \geq 100$ GeV. The allowed regions of large $m_{h_{1,2}^\pm}$ at TeV scale corresponding to $(g-2)_\mu$ experimental data may be tested indirectly through the process $\mu^+\mu^- \to \gamma^* \to h\gamma$ at multi-TeV muon colliders [99].

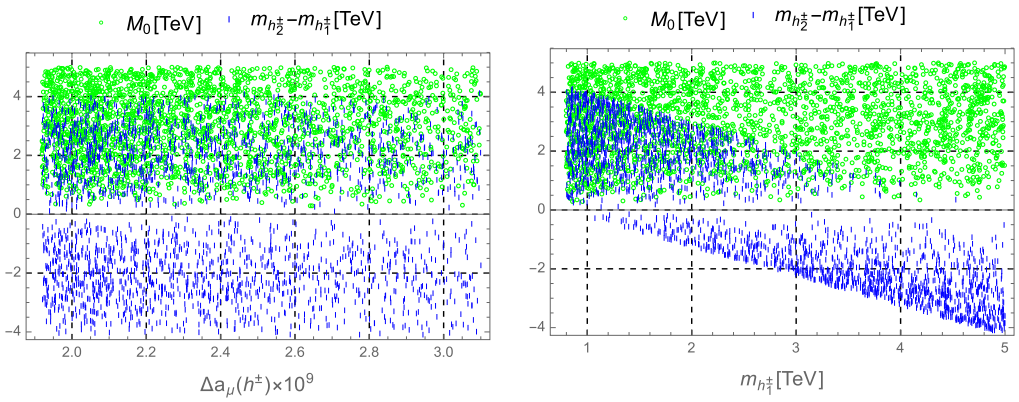

Fig. 5. The correlations of $\Delta a_\mu(h^\pm)$ and $m_{h_1^\pm}$ vs. masses M_0 and $m_{h_{1,2}^\pm}$ with $f_H = t_\beta^{-1}$.

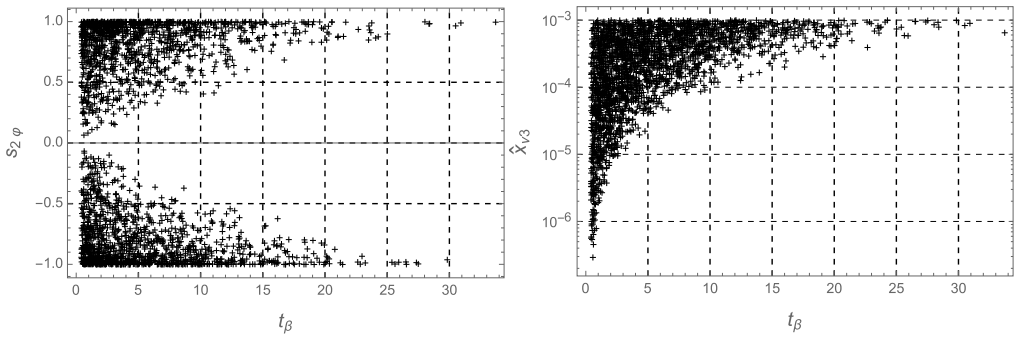

Fig. 6. The correlations of t_β vs other free parameters in the allowed regions with $f_H = t_\beta^{-1}$.

Finally, the correlations showing significant dependence of free parameters and t_β are given in Fig. 6, where the allowed regions with large $t_\beta \geq 20$ require both conditions of large mixing $|s_{2\varphi}| = 1$ and large $\hat{x}_{v3}$. We obtain a small allowed range of $t_\beta \leq 10$ that was missed in Ref. [55]. Our result is consistent with the discussion corresponding to 3-3-1 models given in Ref. [93,101], where the THDM is embedded.

For the case of $f_H = (-t_\beta)$, i.e., RH neutrino and charged leptons singlets couple with the same $SU(2)_L$ Higgs doublet Φ_1 in Yukawa Lagrangian (6), for example Ref. [101]. Then large $a_{e_a}(h^\pm)$ in Eq. (39) support large t_β. In addition, even when $a_{e_a}(h^\pm) \sim s_{2\varphi} \neq 0$, the first terms in the first lines of Eq. (34) or (35) may be large enough consistent with $\Delta a_{\mu,e}^{\rm NP}$ in both sign and amplitude. But the simple assumptions of the couplings and the total neutrino mass matrix in this work are not enough to explain both $(g-2)_{e,\mu}$ experimental data. The perturbative constraint gives an upper bound on M_0, namely

$$M_0 \left|\left(\hat{x}_\nu^{1/2} U_{\rm PMNS}^\dagger\right)_{ab}\right| = \frac{v c_\beta}{\sqrt{2}} \left|(Y_1^N)_{(a+3)b}\right| \Rightarrow M_0 < \hat{x}_{\nu,3}^{-1/2} \left|U_{\rm PMNS,23}\right|^{-1} v c_\beta \sqrt{2\pi}, \quad (42)$$

therefore M_0 may be small with small c_β equivalently with large t_β. We always have $M_0 <$ 1.6 TeV for $t_\beta = 0.4$ and $\hat{x}_{\nu,3} = 10^{-3}$. Although $t_\beta \geq 0.4$ is always kept, smaller $\hat{x}_{\nu,3} \leq 10^{-3}$ may allow large M_0 which also allow large $m_{h_{1,2}^\pm}$. On the other hand, from Eq. (39), $|a_{e_a}| \sim$

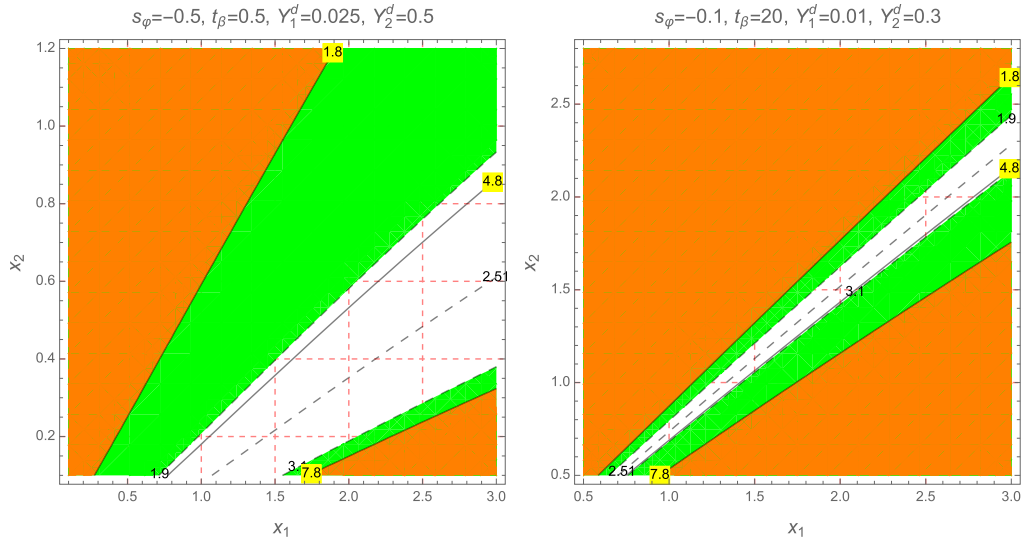

Fig. 7. Contour plots of $\Delta a_\mu(h^\pm) \times 10^9$ and $\Delta a_e(h^\pm) \times 10^{13}$ as functions of x_1 and x_2, where $\hat{x}_{v3} = 5 \times 10^{-4}$ and $f_H = -t_\beta$. The green (orange) regions are excluded by the 1σ data of $\Delta a_\mu^{\rm NP}$ ($\Delta a_e^{\rm NP}$). The black and dashed-black curves show the constant values of $\Delta a_e(h^\pm) \times 10^{13}$ and $\Delta a_\mu(h^\pm) \times 10^9$, respectively.

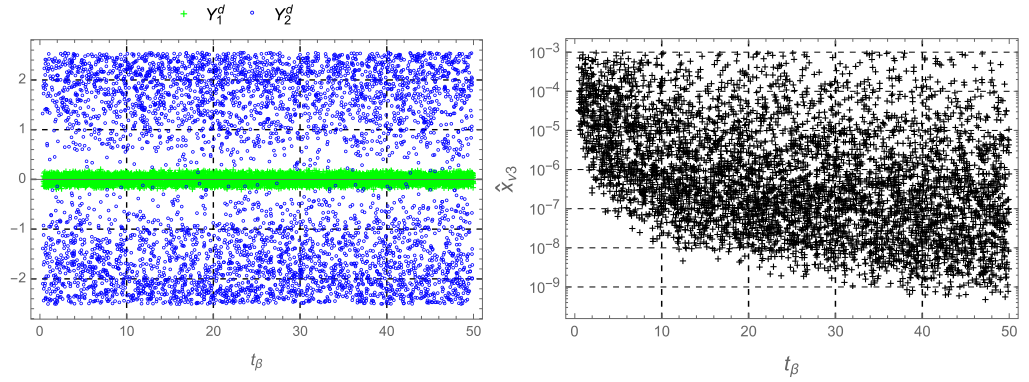

Fig. 8. The correlations of t_β vs other free parameters in the allowed regions with $f_H = -t_\beta$.

$t_\beta\,(x_{v3})^{1/2}\,|s_{2\varphi} Y_a^d|$, hence the allowed regions are easily satisfied for small t_β and large values of other parameters. Our numerical analysis shows that large $x_{v3} \geq 10^{-4}$ allows all $t_\beta \leq 50$ and all singly charged Higgs masses at the TeV scale. Contour plots of $\Delta a_\mu(h^\pm) \times 10^9$ and $\Delta a_e(h^\pm) \times 10^{13}$ for $\hat{x}_{v,3} = 5 \times 10^{-4}$ with small $t_\beta = 0.5$ and large $t_\beta = 20$ are shown in Fig. 7.

Regarding the numerical analysis in the scanning range (41) with $f_H = -t_\beta$, the allowed ranges are tighter than the scanning regions as shown below

$$|s_\varphi| > 10^{-3},\ 0.21 \geq |Y_1^d| > 0.002,\ 2.6 > |Y_2^d| > 0.02,\ \hat{x}_{v3} > 3 \times 10^{-10}. \tag{43}$$

In addition small $M_0 \leq 30$ GeV is also allowed. The numerical results of the correlations between t_β vs. Y_1^d, Y_2^d, and $\hat{x}_{v3}$ are shown in Fig. 8, where the allowed ranges of Y_2^d correspond to a rather narrow allowed range of Y_1^d, see Eq. (43). This implies that the phenomenology of the

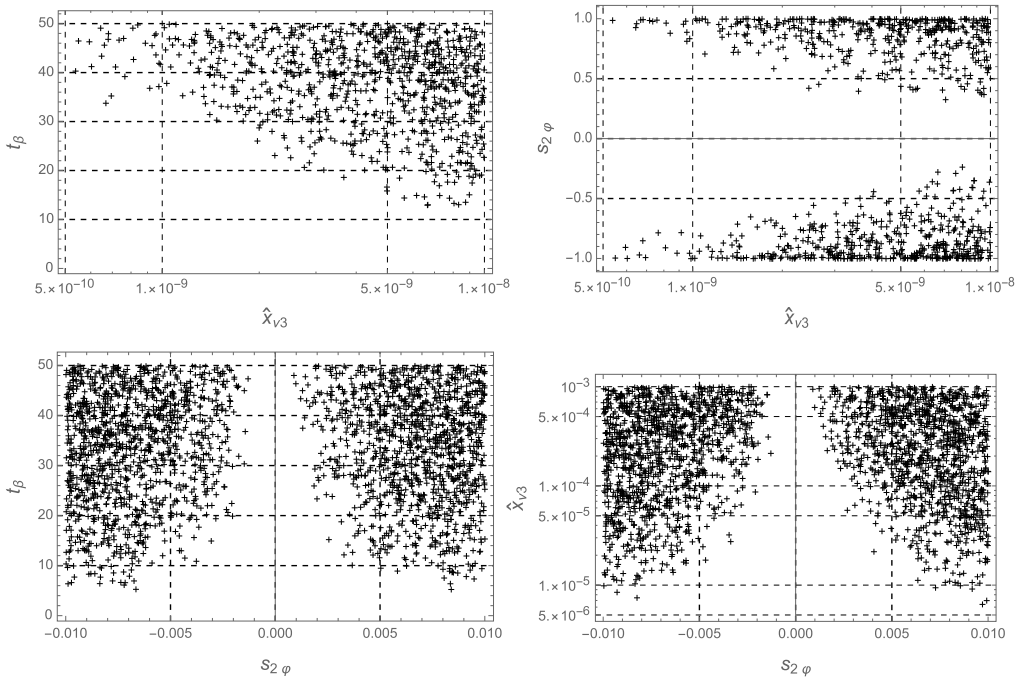

Fig. 9. The correlations of t_β vs $s_{2\varphi}$ (upper panels) and $\hat{x}_{\nu 3}$ (lower panels) near lower bounds of their allowed ranges with $f_H = -t_\beta$.

singly charged Higgs boson at colliders related with these two couplings will have some certain relations that should be experimentally verified.

We have checked numerically that although lower bounds for allowed ranges of s_φ and $\hat{x}_{\nu 3}$ are tiny, but never vanishes. In addition, small allowed values of $\hat{x}_{\nu 3}$ near lower bounds require both large $t_\beta \to 50$ and $|s_{2\varphi}| = 2|c_\varphi s_\varphi| \to 1$, implying the existence of $\Delta a_{e_{a,0}}(h^\pm)$. Also, small allowed values of $|s_{2\varphi}|$ near the lower bound require both large $\hat{x}_{\nu 3} \to 10^{-3}$ and t_β. Illustrations for these comments are shown in Fig. 9. We see also that, the relation shown in Fig. 4 is also true with $f_H = -t_\beta$.

Finally, we have comments regarding the $(g-2)_e$ data [26]: $\Delta a_e^{\rm NP} = -(8.7 \pm 3.6) \times 10^{-13}$. The allowed regions of parameter space corresponding to this data can be derived from the above described numerical analysis. Namely, excepting Y_1^d all allowed ranges of free parameters are kept unchanged to guarantee consistency with the experimental $(g-2)_\mu$ data. On the other hand, Y_1^d is changed into new values such that $Y_1^d \to \frac{(-8.7\pm 3.6)}{(4.8\pm 3)} \times Y_2^d$ and exclude too large values violating the perturbative limit. The two models under consideration predict allowed regions of parameter space that are different from those discussed in Ref. [59,112] for the THDM model where fermions couple to two Higgs doublets with the aligned assumption of the two respective Yukawa couplings $Y'_{2f} = \zeta_f Y'_{1f}$ with $f = u, d, \ell, \nu$, where ν denote new right handed neutrinos ν_{aR}. The large contributions to $(g-2)_\mu$ come from the two-loop Barr-Zee contributions with the necessary condition of very light neutral CP-odd Higgs boson mass, $m_A \leq 60$ GeV. On the other hand, large and negative sign of $(g-2)_e$ satisfying the 1σ experimental data comes from one-loop contribution with the condition that $\zeta_\ell \zeta_\nu < 0$. The model in Ref. [59] does not include the case $Y'_{1\nu} = 0$ and $Y'_{2\nu} \neq 0$, corresponding to $f_H = t_\beta^{-1}$ mentioned in our work. In addition, the

region of parameter space with $\zeta_\nu = \zeta_\ell = 0$ corresponding to $f_H = -t_\beta$ is excluded by the 1σ range of $(g-2)_e$ data. In contrast, our models always assume that $Y'_{1u} = \zeta_\ell = 0$, and only one of the two Yukawa coupling matrices $Y'_{1\nu}$ or $Y'_{2\nu}$ being non-zero. The Yukawa couplings Y^d_a between only gauge singlets $N_{a(b+3)} e_{aR} h^+$ give main one-loop contributions to both $\Delta a_{e,\mu}$, leading to nearly linear relations of these two quantities. Finally, our models predict regions of parameter space that successfully accommodate the experimental data on both $(g-2)_{e,\mu}$ anomalies without the requirement of small m_A and rather light $m_{h^\pm_k} \sim \mathcal{O}(10^2)$ GeV. Therefore, our models will be a another solution for the $(g-2)_{e,\mu}$ anomalies if a light CP odd scalar A is excluded by future experiments.

4. Conclusion

In this work we have shown that the appearance of heavy ISS neutrinos and singly charged Higgs bosons is a very promoting solution to explain the experimental data on both $(g-2)_{\mu,e}$ anomalies in many different types of THDM, and in regions of parameter space allowing heavy singly charged Higgs boson masses up to the TeV scale and small values of the $\tan\beta$ parameter satisfying $\tan\beta \geq 0.4$. In particularly, the most important terms $\Delta a_{e_a,0}$ given in Eq. (39) are enough to explain successfully the experimental AMM data of both a_e and a_μ in THDM, including the model type I, where other loop contributions to Δa_{e_a} caused by power of factor t_β^{-1} are suppressed. In other types of THDM needing large t_β giving sizeable loop contributions to Δa_{e_a}, light masses of new Higgs bosons around few hundred GeV in the loop are also necessary to successfully accommodate the recent experimental AMM data. The presence of $\Delta a_{e_a,0}$ is an alternative way to explain the AMM data if light mass ranges are excluded by future collider searches. This solution will enlarge the allowed regions of parameter spaces of the THDM which can simultaneously explain the $(g-2)_{e,\mu}$ data thanks to the one loop exchange of electrically charged Higgs bosons with masses within the LHC reach. The existence of $\Delta a_{e_a,0}$ also yields the following consequences: i) the non-zero mixing $s_{2\varphi} \neq 0$, ii) the non-unitary parameter $\hat{x}_{\nu,3}$ has a lower bound $\hat{x}_{\nu,3} \geq 4 \times 10^{-7}$ for $f_H = t_\beta^{-1}$ and $\hat{x}_{\nu,3} \geq \mathcal{O}(10^{-10})$ for $f_H = -t_\beta$, iii) and lower bounds of new heavy neutrino masses are of the order of $\mathcal{O}(100)$ GeV. Tiny but non vanishing values of $\hat{x}_{\nu,3} \sim 10^{-10}$ require very large t_β and $|s_{2\varphi}| \to 1$. Despite the large number of parameters, the model is economical with a small amount of BSM fields, much lower than the corresponding to several models considered in the literature. Besides that, apart from explaining the $(g-2)$ anomalies, the model considered in this paper can feature interesting collider signatures mainly related with electrically charged scalar and heavy neutrino production at the LHC, that can be useful to test that theory at colliders.

CRediT authorship contribution statement

L.T. Hue: Formal analysis, Investigation, Writing – original draft. **A.E. Cárcamo Hernández:** Writing – review & editing. **H.N. Long:** Writing – review & editing. **T.T. Hong:** Formal analysis, Investigation.

Declaration of competing interest

The authors declare that they have no known competing financial interests or personal relationships that could have appeared to influence the work reported in this paper.

Data availability

The data that has been used is confidential.

Acknowledgements

We thank Prof. Ray Volkas, Dr. Claudio Andrea, Dr. Lei Wang, and Dr. Wen Yin for useful comments. L. T. Hue is thankful to Van Lang University. This research is funded by the Vietnam National Foundation for Science and Technology Development (NAFOSTED) under the grant number 103.01-2019.387 as well as by ANID-Chile FONDECYT 1210378, ANID PIA/APOYO AFB180002, and Milenio-ANID-ICN2019_044.

References

[1] B. Abi, et al., Muon g-2, Phys. Rev. Lett. 126 (2021) 141801, arXiv:2104.03281 [hep-ex].
[2] G.W. Bennett, et al., Muon g-2, Phys. Rev. D 73 (2006) 072003, arXiv:hep-ex/0602035 [hep-ex].
[3] T. Aoyama, N. Asmussen, M. Benayoun, J. Bijnens, T. Blum, M. Bruno, I. Caprini, C.M. Carloni Calame, M. Cè, G. Colangelo, et al., Phys. Rep. 887 (2020) 1, arXiv:2006.04822 [hep-ph].
[4] A. Keshavarzi, D. Nomura, T. Teubner, Phys. Rev. D 97 (11) (2018) 114025, arXiv:1802.02995 [hep-ph].
[5] G. Colangelo, M. Hoferichter, P. Stoffer, J. High Energy Phys. 02 (2019) 006, arXiv:1810.00007 [hep-ph].
[6] M. Hoferichter, B.L. Hoid, B. Kubis, J. High Energy Phys. 08 (2019) 137, arXiv:1907.01556 [hep-ph].
[7] M. Davier, A. Hoecker, B. Malaescu, Z. Zhang, Eur. Phys. J. C 80 (3) (2020) 241, Erratum: Eur. Phys. J. C 80 (5) (2020) 410, arXiv:1908.00921 [hep-ph].
[8] A. Keshavarzi, D. Nomura, T. Teubner, Phys. Rev. D 101 (1) (2020) 014029, arXiv:1911.00367 [hep-ph].
[9] A. Kurz, T. Liu, P. Marquard, M. Steinhauser, Phys. Lett. B 734 (2014) 144–147, arXiv:1403.6400 [hep-ph].
[10] K. Melnikov, A. Vainshtein, Phys. Rev. D 70 (2004) 113006, arXiv:hep-ph/0312226 [hep-ph].
[11] P. Masjuan, P. Sanchez-Puertas, Phys. Rev. D 95 (5) (2017) 054026, arXiv:1701.05829 [hep-ph].
[12] G. Colangelo, M. Hoferichter, M. Procura, P. Stoffer, J. High Energy Phys. 04 (2017) 161, arXiv:1702.07347 [hep-ph].
[13] M. Hoferichter, B.L. Hoid, B. Kubis, S. Leupold, S.P. Schneider, J. High Energy Phys. 10 (2018) 141, arXiv:1808.04823 [hep-ph].
[14] A. Gérardin, H.B. Meyer, A. Nyffeler, Phys. Rev. D 100 (3) (2019) 034520, arXiv:1903.09471 [hep-lat].
[15] J. Bijnens, N. Hermansson-Truedsson, A. Rodríguez-Sánchez, Phys. Lett. B 798 (2019) 134994, arXiv:1908.03331 [hep-ph].
[16] G. Colangelo, F. Hagelstein, M. Hoferichter, L. Laub, P. Stoffer, J. High Energy Phys. 03 (2020) 101, arXiv:1910.13432 [hep-ph].
[17] G. Colangelo, M. Hoferichter, A. Nyffeler, M. Passera, P. Stoffer, Phys. Lett. B 735 (2014) 90–91, arXiv:1403.7512 [hep-ph].
[18] T. Blum, N. Christ, M. Hayakawa, T. Izubuchi, L. Jin, C. Jung, C. Lehner, Phys. Rev. Lett. 124 (13) (2020) 132002, arXiv:1911.08123 [hep-lat].
[19] T. Aoyama, M. Hayakawa, T. Kinoshita, M. Nio, Phys. Rev. Lett. 109 (2012) 111808, arXiv:1205.5370 [hep-ph].
[20] T. Aoyama, T. Kinoshita, M. Nio, Atoms 7 (1) (2019) 28.
[21] A. Czarnecki, W.J. Marciano, A. Vainshtein, Phys. Rev. D 67 (2003) 073006, Erratum: Phys. Rev. D 73 (2006) 119901, arXiv:hep-ph/0212229 [hep-ph].
[22] C. Gnendiger, D. Stöckinger, H. Stöckinger-Kim, Phys. Rev. D 88 (2013) 053005, arXiv:1306.5546 [hep-ph].
[23] M. Davier, A. Hoecker, B. Malaescu, Z. Zhang, Eur. Phys. J. C 77 (12) (2017) 827, arXiv:1706.09436 [hep-ph].
[24] M. Davier, A. Hoecker, B. Malaescu, Z. Zhang, Eur. Phys. J. C 71 (2011) 1515, Erratum: Eur. Phys. J. C 72 (2012) 1874, arXiv:1010.4180 [hep-ph].
[25] D. Hanneke, S. Fogwell, G. Gabrielse, Phys. Rev. Lett. 100 (2008) 120801, arXiv:0801.1134 [physics.atom-ph].
[26] R.H. Parker, C. Yu, W. Zhong, B. Estey, H. Müller, Science 360 (2018) 191, arXiv:1812.04130 [physics.atom-ph].
[27] L. Morel, Z. Yao, P. Cladé, S. Guellati-Khélifa, Nature 588 (7836) (2020) 61–65.
[28] T. Aoyama, M. Hayakawa, T. Kinoshita, M. Nio, Phys. Rev. Lett. 109 (2012) 111807, arXiv:1205.5368 [hep-ph].
[29] S. Laporta, Phys. Lett. B 772 (2017) 232–238, arXiv:1704.06996 [hep-ph].
[30] T. Aoyama, T. Kinoshita, M. Nio, Phys. Rev. D 97 (3) (2018) 036001, arXiv:1712.06060 [hep-ph].

[31] H. Terazawa, Nonlinear Phenom. Complex Syst. 21 (3) (2018) 268–272.
[32] S. Volkov, Phys. Rev. D 100 (9) (2019) 096004, arXiv:1909.08015 [hep-ph].
[33] A. Gérardin, Eur. Phys. J. A 57 (4) (2021) 116, arXiv:2012.03931 [hep-lat].
[34] R. Dermisek, A. Raval, Phys. Rev. D 88 (2013) 013017, arXiv:1305.3522 [hep-ph].
[35] A. Crivellin, M. Hoferichter, P. Schmidt-Wellenburg, Phys. Rev. D 98 (11) (2018) 113002, arXiv:1807.11484 [hep-ph].
[36] P. Escribano, J. Terol-Calvo, A. Vicente, Phys. Rev. D 103 (11) (2021) 115018, arXiv:2104.03705 [hep-ph].
[37] A. Crivellin, M. Hoferichter, J. High Energy Phys. 07 (2021) 135, arXiv:2104.03202 [hep-ph].
[38] R. Dermisek, K. Hermanek, N. McGinnis, Phys. Rev. D 104 (5) (2021) 055033, arXiv:2103.05645 [hep-ph].
[39] A.E.C. Hernández, S.F. King, H. Lee, Phys. Rev. D 103 (11) (2021) 115024, arXiv:2101.05819 [hep-ph].
[40] E.J. Chun, T. Mondal, J. High Energy Phys. 11 (2020) 077, arXiv:2009.08314 [hep-ph].
[41] M. Frank, I. Saha, Phys. Rev. D 102 (11) (2020) 115034, arXiv:2008.11909 [hep-ph].
[42] K.F. Chen, C.W. Chiang, K. Yagyu, J. High Energy Phys. 09 (2020) 119, arXiv:2006.07929 [hep-ph].
[43] P.M. Ferreira, B.L. Gonçalves, F.R. Joaquim, M. Sher, Phys. Rev. D 104 (5) (2021) 053008, arXiv:2104.03367 [hep-ph].
[44] M. Endo, S. Mishima, J. High Energy Phys. 08 (08) (2020) 004, arXiv:2005.03933 [hep-ph].
[45] C. Hati, J. Kriewald, J. Orloff, A.M. Teixeira, J. High Energy Phys. 07 (2020) 235, arXiv:2005.00028 [hep-ph].
[46] D. Borah, M. Dutta, S. Mahapatra, N. Sahu, Phys. Rev. D 105 (1) (2022) 015029, arXiv:2109.02699 [hep-ph].
[47] H. Bharadwaj, S. Dutta, A. Goyal, J. High Energy Phys. 11 (2021) 056, arXiv:2109.02586 [hep-ph].
[48] A.S. De Jesus, S. Kovalenko, F.S. Queiroz, C. Siqueira, K. Sinha, Phys. Rev. D 102 (3) (2020) 035004, arXiv:2004.01200 [hep-ph].
[49] D. Cogollo, Y.M. Oviedo-Torres, Y.S. Villamizar, Int. J. Mod. Phys. A 35 (23) (2020) 2050126, arXiv:2004.14792 [hep-ph].
[50] B.D. Sáez, K. Ghorbani, Phys. Lett. B 823 (2021) 136750, arXiv:2107.08945 [hep-ph].
[51] I. Bigaran, R.R. Volkas, Phys. Rev. D 102 (2020) 075037, arXiv:2002.12544 [hep-ph].
[52] A. Crivellin, D. Mueller, F. Saturnino, Phys. Rev. Lett. 127 (2) (2021) 021801, arXiv:2008.02643 [hep-ph].
[53] D. Zhang, J. High Energy Phys. 07 (2021) 069, arXiv:2105.08670 [hep-ph].
[54] W.Y. Keung, D. Marfatia, P.Y. Tseng, LHEP 2021 (2021) 209, arXiv:2104.03341 [hep-ph].
[55] T. Mondal, H. Okada, Nucl. Phys. B 976 (2022) 115716, arXiv:2103.13149 [hep-ph].
[56] D.W. Kang, J. Kim, H. Okada, Phys. Lett. B 822 (2021) 136666, arXiv:2107.09960 [hep-ph].
[57] A.E. Cárcamo Hernández, C. Espinoza, J. Carlos Gómez-Izquierdo, M. Mondragón, arXiv:2104.02730 [hep-ph].
[58] S.P. Li, X.Q. Li, Y.Y. Li, Y.D. Yang, X. Zhang, J. High Energy Phys. 01 (2021) 034, arXiv:2010.02799 [hep-ph].
[59] L. Delle Rose, S. Khalil, S. Moretti, Phys. Lett. B 816 (2021) 136216, arXiv:2012.06911 [hep-ph].
[60] F.J. Botella, F. Cornet-Gomez, M. Nebot, Phys. Rev. D 102 (3) (2020) 035023, arXiv:2006.01934 [hep-ph].
[61] X.F. Han, T. Li, H.X. Wang, L. Wang, Y. Zhang, Phys. Rev. D 104 (11) (2021) 115001, arXiv:2104.03227 [hep-ph].
[62] C.H. Chen, C.W. Chiang, T. Nomura, Phys. Rev. D 104 (5) (2021) 055011, arXiv:2104.03275 [hep-ph].
[63] X.F. Han, T. Li, L. Wang, Y. Zhang, Phys. Rev. D 99 (9) (2019) 095034, arXiv:1812.02449 [hep-ph].
[64] M. Aoki, S. Kanemura, K. Tsumura, K. Yagyu, Phys. Rev. D 80 (2009) 015017, arXiv:0902.4665 [hep-ph].
[65] A. Jueid, J. Kim, S. Lee, J. Song, Phys. Rev. D 104 (9) (2021) 095008, arXiv:2104.10175 [hep-ph].
[66] P. Athron, C. Balázs, D.H. Jacob, W. Kotlarski, D. Stöckinger, H. Stöckinger-Kim, J. High Energy Phys. 09 (2021) 080, arXiv:2104.03691 [hep-ph].
[67] M. Badziak, K. Sakurai, J. High Energy Phys. 10 (2019) 024, arXiv:1908.03607 [hep-ph].
[68] S. Li, Y. Xiao, J.M. Yang, Eur. Phys. J. C 82 (3) (2022) 276, arXiv:2107.04962 [hep-ph].
[69] M. Endo, W. Yin, J. High Energy Phys. 08 (2019) 122, arXiv:1906.08768 [hep-ph].
[70] B. Dutta, S. Ghosh, T. Li, Phys. Rev. D 102 (5) (2020) 055017, arXiv:2006.01319 [hep-ph].
[71] A.E. Cárcamo Hernández, S. Kovalenko, R. Pasechnik, I. Schmidt, J. High Energy Phys. 06 (2019) 056, arXiv:1901.02764 [hep-ph].
[72] A.E.C. Hernández, D.T. Huong, I. Schmidt, Eur. Phys. J. C 82 (1) (2022) 63, arXiv:2109.12118 [hep-ph].
[73] A.E. Cárcamo Hernández, S. Kovalenko, R. Pasechnik, I. Schmidt, Eur. Phys. J. C 79 (7) (2019) 610, arXiv:1901.09552 [hep-ph].
[74] R. Adhikari, I.A. Bhat, D. Borah, E. Ma, D. Nanda, Phys. Rev. D 105 (3) (2022) 035006, arXiv:2109.05417 [hep-ph].
[75] J. Herrero-García, T. Ohlsson, S. Riad, J. Wirén, J. High Energy Phys. 04 (2017) 130, arXiv:1701.05345 [hep-ph].
[76] S. Davidson, H.E. Haber, Phys. Rev. D 72 (2005) 035004, Erratum: Phys. Rev. D 72 (2005) 099902, arXiv:hep-ph/0504050 [hep-ph].
[77] L. Allwicher, P. Arnan, D. Barducci, M. Nardecchia, J. High Energy Phys. 10 (2021) 129, arXiv:2108.00013 [hep-ph].

[78] A. Ibarra, E. Molinaro, S.T. Petcov, J. High Energy Phys. 09 (2010) 108, arXiv:1007.2378 [hep-ph].
[79] P.A. Zyla, et al., Particle Data Group, PTEP 2020 (2020) 083C01.
[80] E. Arganda, M.J. Herrero, X. Marcano, C. Weiland, Phys. Rev. D 91 (2015) 015001, arXiv:1405.4300 [hep-ph].
[81] J.A. Casas, A. Ibarra, Nucl. Phys. B 618 (2001) 171, arXiv:hep-ph/0103065 [hep-ph].
[82] A.M. Baldini, et al., MEG, Eur. Phys. J. C 76 (8) (2016) 434, arXiv:1605.05081 [hep-ex].
[83] B. Aubert, et al., BaBar, Phys. Rev. Lett. 104 (2010) 021802, arXiv:0908.2381 [hep-ex].
[84] N. Aghanim, et al., Planck, Astron. Astrophys. 641 (2020) A6, Erratum: Astron. Astrophys. 652 (2021) C4, arXiv:1807.06209 [astro-ph.CO].
[85] J.P. Pinheiro, C.A. de, S. Pires, F.S. Queiroz, Y.S. Villamizar, Phys. Lett. B 823 (2021) 136764, arXiv:2107.01315 [hep-ph].
[86] E. Fernandez-Martinez, J. Hernandez-Garcia, J. Lopez-Pavon, J. High Energy Phys. 08 (2016) 033, arXiv:1605.08774 [hep-ph].
[87] N.R. Agostinho, G.C. Branco, P.M.F. Pereira, M.N. Rebelo, J.I. Silva-Marcos, Eur. Phys. J. C 78 (11) (2018) 895, arXiv:1711.06229 [hep-ph].
[88] T.N. Dao, M. Mühlleitner, A.V. Phan, Eur. Phys. J. C 82 (8) (2022) 667, arXiv:2108.10088 [hep-ph].
[89] C. Biggio, E. Fernandez-Martinez, M. Filaci, J. Hernandez-Garcia, J. Lopez-Pavon, J. High Energy Phys. 05 (2020) 022, arXiv:1911.11790 [hep-ph].
[90] A.M. Coutinho, A. Crivellin, C.A. Manzari, Phys. Rev. Lett. 125 (7) (2020) 071802, arXiv:1912.08823 [hep-ph].
[91] C.A. Manzari, A.M. Coutinho, A. Crivellin, PoS LHCP2020 (2021) 242, arXiv:2009.03877 [hep-ph].
[92] F. Jegerlehner, A. Nyffeler, Phys. Rep. 477 (2009) 1–110, arXiv:0902.3360 [hep-ph].
[93] A. Nepomuceno, B. Meirose, Phys. Rev. D 101 (2020) 035017, arXiv:1911.12783 [hep-ph].
[94] A. Das, N. Okada, Phys. Rev. D 88 (2013) 113001, arXiv:1207.3734 [hep-ph].
[95] A. Das, P.S. Bhupal Dev, N. Okada, Phys. Lett. B 735 (2014) 364–370, arXiv:1405.0177 [hep-ph].
[96] A. Das, N. Okada, Phys. Rev. D 93 (3) (2016) 033003, arXiv:1510.04790 [hep-ph].
[97] A. Das, P. Konar, S. Majhi, J. High Energy Phys. 06 (2016) 019, arXiv:1604.00608 [hep-ph].
[98] A. Das, S. Jana, S. Mandal, S. Nandi, Phys. Rev. D 99 (5) (2019) 055030, arXiv:1811.04291 [hep-ph].
[99] W. Yin, M. Yamaguchi, Phys. Rev. D 106 (3) (2022) 033007, arXiv:2012.03928 [hep-ph].
[100] L.T. Hue, K.H. Phan, T.P. Nguyen, H.N. Long, H.T. Hung, Eur. Phys. J. C 82 (8) (2022) 722, arXiv:2109.06089 [hep-ph].
[101] L.T. Hue, H.T. Hung, N.T. Tham, H.N. Long, T.P. Nguyen, Phys. Rev. D 104 (2021) 033007, arXiv:2104.01840 [hep-ph].
[102] J. Schechter, J.W.F. Valle, Phys. Rev. D 25 (1982) 774.
[103] J.G. Korner, A. Pilaftsis, K. Schilcher, Phys. Rev. D 47 (1993) 1080–1086, arXiv:hep-ph/9301289 [hep-ph].
[104] W. Grimus, L. Lavoura, J. High Energy Phys. 11 (2000) 042, arXiv:hep-ph/0008179 [hep-ph].
[105] E. Ma, Phys. Rev. D 73 (2006) 077301, arXiv:hep-ph/0601225 [hep-ph].
[106] G. Degrassi, S. Di Vita, J. Elias-Miro, J.R. Espinosa, G.F. Giudice, G. Isidori, A. Strumia, J. High Energy Phys. 08 (2012) 098, arXiv:1205.6497 [hep-ph].
[107] S. Jangid, P. Bandyopadhyay, Eur. Phys. J. C 80 (8) (2020) 715, arXiv:2003.11821 [hep-ph].
[108] S. Jangid, P. Bandyopadhyay, P.S. Bhupal Dev, A. Kumar, J. High Energy Phys. 08 (2020) 154, arXiv:2001.01764 [hep-ph].
[109] C. Coriano, L. Delle Rose, C. Marzo, J. High Energy Phys. 02 (2016) 135, arXiv:1510.02379 [hep-ph].
[110] L. Delle Rose, C. Marzo, A. Urbano, J. High Energy Phys. 12 (2015) 050, arXiv:1506.03360 [hep-ph].
[111] P. Bandyopadhyay, S. Jangid, M. Mitra, J. High Energy Phys. 02 (2021) 075, arXiv:2008.11956 [hep-ph].
[112] L.D. Rose, S. Khalil, S. Moretti, arXiv:2111.12185 [hep-ph].
[113] J. de Blas, EPJ Web Conf. 60 (2013) 19008, arXiv:1307.6173 [hep-ph].
[114] P. Bandyopadhyay, E.J. Chun, H. Okada, J.C. Park, J. High Energy Phys. 01 (2013) 079, arXiv:1209.4803 [hep-ph].
[115] J. Calle, D. Restrepo, Ó. Zapata, Phys. Rev. D 104 (1) (2021) 1, arXiv:2103.15328 [hep-ph].